8. Tanaka, T., N. Kato, M. J. Cho, K. Sugiyama, and K. Shimotohno. 1996. Structure of the 3′ terminus of the hepatitis C virus genome. *J. Virol.* **70:** 3307–3312.
9. McLauchlan, J. 2009. Lipid droplets and hepatitis C virus infection. *Biochim. Biophys. Acta.* **1791:** 552–559.
10. Bartenschlager, R., F. Penin, V. Lohmann, and P. André. 2011. Assembly of infectious hepatitis C virus particles. *Trends Microbiol.* **19:** 95–103.
11. Negro, F. 2010. Abnormalities of lipid metabolism in hepatitis C virus infection. *Gut.* **59:** 1279–1287.
12. Herker, E., and M. Ott. 2011. Unique ties between hepatitis C virus replication and intracellular lipids. *Trends Endocrinol. Metab.* **22:** 241–248.
13. Ploss, A., and M. J. Evans. 2012. Hepatitis C virus host cell entry. *Curr. Opin. Virol.* **2:** 14–19.
14. Moriya, K., H. Yotsuyanagi, Y. Shintani, H. Fujie, K. Ishibashi, Y. Matsuura, T. Miyamura, and K. Koike. 1997. Hepatitis C virus core protein induces hepatic steatosis in transgenic mice. *J. Gen. Virol.* **78:** 1527–1531.
15. Moradpour, D., C. Englert, T. Wakita, and J. R. Wands. 1996. Characterization of cell lines allowing tightly regulated expression of hepatitis C virus core protein. *Virology.* **222:** 51–63.
16. Jirasko, V., R. Montserret, J. Y. Lee, J. Gouttenoire, D. Moradpour, F. Penin, and R. Bartenschlager. 2010. Structural and functional studies of nonstructural protein 2 of the hepatitis C virus reveal its key role as organizer of virion assembly. *PLoS Pathog.* **6:** e1001233.
17. Shi, S. T., S. J. Polyak, H. Tu, D. R. Taylor, D. R. Gretch, and M. M. Lai. 2002. Hepatitis C virus NS5A colocalizes with the core protein on lipid droplets and interacts with apolipoproteins. *Virology.* **292:** 198–210.
18. Roingeard, P., C. Hourioux, E. Blanchard, and G. Prensier. 2008. Hepatitis C virus budding at lipid droplet-associated ER membrane visualized by 3D electron microscopy. *Histochem. Cell Biol.* **130:** 561–566.
19. Christianson, J. L., E. Boutet, V. Puri, A. Chawla, and M. P. Czech. 2010. Identification of the lipid droplet targeting domain of the Cidea protein. *J. Lipid Res.* **51:** 3455–3462.
20. Hinson, E. R., and P. Cresswell. 2009. The antiviral protein, viperin, localizes to lipid droplets via its N-terminal amphipathic alpha-helix. *Proc. Natl. Acad. Sci. USA.* **106:** 20452–20457.
21. Poppelreuther, M., B. Rudolph, C. Du, R. Grossmann, M. Becker, C. Thiele, R. Ehehalt, and J. Fuellekrug. 2012. The N-terminal region of acyl-CoA synthetase 3 is essential for both the localization on lipid droplets and the function in fatty acid uptake. *J. Lipid Res.* **53:** 888–900.
22. Boulant, S., R. Montserret, R. G. Hope, M. Ratinier, P. Targett-Adams, J. P. Lavergne, F. Penin, and J. McLauchlan. 2006. Structural determinants that target the hepatitis C virus core protein to lipid droplets. *J. Biol. Chem.* **281:** 22236–22247.
23. Unterstab, G., R. Gosert, D. Leuenberger, P. Lorentz, C. H. Rinaldo, and H. H. Hirsch. 2010. The polyomavirus BK agnoprotein co-localizes with lipid droplets. *Virology.* **399:** 322–331.
24. Ingelmo-Torres, M., E. Gonzalez-Moreno, A. Kassan, M. Hanzal-Bayer, F. Tebar, A. Herms, T. Grewal, J. F. Hancock, C. Enrich, M. Bosch, et al. 2009. Hydrophobic and basic domains target proteins to lipid droplets. *Traffic.* **10:** 1785–1801.
25. Subramanian, V., A. Garcia, A. Sekowski, and D. L. Brasaemle. 2004. Hydrophobic sequences target and anchor perilipin A to lipid droplets. *J. Lipid Res.* **45:** 1983–1991.
26. Zehmer, J. K., R. Bartz, P. Liu, and R. G. Anderson. 2008. Identification of a novel N-terminal hydrophobic sequence that targets proteins to lipid droplets. *J. Cell Sci.* **121:** 1852–1860.
27. Gouttenoire, J., F. Penin, and D. Moradpour. 2010. Hepatitis C virus nonstructural protein 4B: a journey into unexplored territory. *Rev. Med. Virol.* **20:** 117–129.
28. Hügle, T., F. Fehrmann, E. Bieck, M. Kohara, H. G. Krausslich, C. M. Rice, H. E. Blum, and D. Moradpour. 2001. The hepatitis C virus nonstructural protein 4B is an integral endoplasmic reticulum membrane protein. *Virology.* **284:** 70–81.
29. Egger, D., B. Wölk, R. Gosert, L. Bianchi, H. E. Blum, D. Moradpour, and K. Bienz. 2002. Expression of hepatitis C virus proteins induces distinct membrane alterations including a candidate viral replication complex. *J. Virol.* **76:** 5974–5984.
30. Ferraris, P., E. Beaumont, R. Uzbekov, D. Brand, J. Gaillard, E. Blanchard, and P. Roingeard. Sequential biogenesis of host cell membrane rearrangements induced by hepatitis C virus infection. *Cell. Mol. Life Sci.* Epub ahead of print. November 25, 2012; doi:10.1007/s00018-012-1213-0.
31. Paul, D., I. Romero-Brey, J. Gouttenoire, S. Stoitsova, J. Krijnse-Locker, D. Moradpour, and R. Bartenschlager. 2011. NS4B self-interaction through conserved C-terminal elements is required for the establishment of functional hepatitis C virus replication complexes. *J. Virol.* **85:** 6963–6976.
32. Romero-Brey, I., A. Merz, A. Chiramel, J. Y. Lee, P. Chlanda, U. Haselman, R. Santarella-Mellwig, A. Habermann, S. Hoppe, S. Kallis, et al. 2012. Three-dimensional architecture and biogenesis of membrane structures associated with hepatitis C virus replication. *PLoS Pathog.* **8:** e1003056.
33. Wakita, T., T. Pietschmann, T. Kato, T. Date, M. Miyamoto, Z. Zhao, K. Murthy, A. Habermann, H. G. Krausslich, M. Mizokami, et al. 2005. Production of infectious hepatitis C virus in tissue culture from a cloned viral genome. *Nat. Med.* **11:** 791–796.
34. Ikeda, M., K. Abe, H. Dansako, T. Nakamura, K. Naka, and N. Kato. 2005. Efficient replication of a full-length hepatitis C virus genome, strain O, in cell culture, and development of a luciferase reporter system. *Biochem. Biophys. Res. Commun.* **329:** 1350–1359.
35. Naka, K., M. Ikeda, K. Abe, H. Dansako, and N. Kato. 2005. Mizoribine inhibits hepatitis C virus RNA replication: effect of combination with interferon-alpha. *Biochem. Biophys. Res. Commun.* **330:** 871–879.
36. Ohsaki, Y., T. Maeda, and T. Fujimoto. 2005. Fixation and permeabilization protocol is critical for the immunolabeling of lipid droplet proteins. *Histochem. Cell Biol.* **124:** 445–452.
37. Tanaka, T., T. Ito, M. Furuta, C. Eguchi, H. Toda, E. Wakabayashi-Takai, and K. Kaneko. 2002. In situ phage screening. A method for identification of subnanogram tissue components in situ. *J. Biol. Chem.* **277:** 30382–30387.
38. Fujimoto, Y., J. Onoduka, K. J. Homma, S. Yamaguchi, M. Mori, Y. Higashi, M. Makita, T. Kinoshita, J. Noda, H. Itabe, et al. 2006. Long-chain fatty acids induce lipid droplet formation in a cultured human hepatocyte in a manner dependent of Acyl-CoA synthetase. *Biol. Pharm. Bull.* **29:** 2174–2180.
39. Boleti, H., D. Smirlis, G. Dalagiorgou, E. F. Meurs, S. Christoforidis, and P. Mavromara. 2010. ER targeting and retention of the HCV NS4B protein relies on the concerted action of multiple structural features including its transmembrane domains. *Mol. Membr. Biol.* **27:** 50–74.
40. Gouttenoire, J., R. Montserret, A. Kennel, F. Penin, and D. Moradpour. 2009. An amphipathic alpha-helix at the C terminus of hepatitis C virus nonstructural protein 4B mediates membrane association. *J. Virol.* **83:** 11378–11384.
41. Gouttenoire, J., V. Castet, R. Montserret, N. Arora, V. Raussens, J. M. Ruysschaert, E. Diesis, H. E. Blum, F. Penin, and D. Moradpour. 2009. Identification of a novel determinant for membrane association in hepatitis C virus nonstructural protein 4B. *J. Virol.* **83:** 6257–6268.
42. Turró, S., M. Ingelmo-Torres, J. M. Estanyol, F. Tebar, M. A. Fernandez, C. V. Albor, K. Gaus, T. Grewal, C. Enrich, and A. Pol. 2006. Identification and characterization of associated with lipid droplet protein 1: A novel membrane-associated protein that resides on hepatic lipid droplets. *Traffic.* **7:** 1254–1269.
43. Lundin, M., M. Monné, A. Widell, G. Von Heijne, and M. A. Persson. 2003. Topology of the membrane-associated hepatitis C virus protein NS4B. *J. Virol.* **77:** 5428–5438.
44. Gouttenoire, J., P. Roingeard, F. Penin, and D. Moradpour. 2010. Amphipathic alpha-helix AH2 is a major determinant for the oligomerization of hepatitis C virus nonstructural protein 4B. *J. Virol.* **84:** 12529–12537.
45. Aligo, J., S. A. Z. Jia, D. Manna, and K. V. Konan. 2009. Formation and function of hepatitis C virus replication complexes require residues in the carboxy-terminal domain of NS4B protein. *Virology.* **393:** 68–83.
46. Brass, V., J. M. Berke, R. Montserret, H. E. Blum, F. Penin, and D. Moradpour. 2008. Structural determinants for membrane association and dynamic organization of the hepatitis C virus NS3-4A complex. *Proc. Natl. Acad. Sci. USA.* **105:** 14545–14550.
47. Gastaminza, P., K. A. Dryden, B. Boyd, M. R. Wood, M. Law, M. Yeager, and F. V. Chisari. 2010. Ultrastructural and biophysical characterization of hepatitis C virus particles produced in cell culture. *J. Virol.* **84:** 10999–11009.
48. Lundin, M., H. Lindström, C. Grönwall, and M. A. Persson. 2006. Dual topology of the processed hepatitis C virus protein NS4B is influenced by the NS5A protein. *J. Gen. Virol.* **87:** 3263–3272.
49. Dimitrova, M., I. Imbert, M. P. Kieny, and C. Schuster. 2003. Protein-protein interactions between hepatitis C virus nonstructural proteins. *J. Virol.* **77:** 5401–5414.
50. Einav, S., M. Elazar, T. Danieli, and J. S. Glenn. 2004. A nucleotide binding motif in hepatitis C virus (HCV) NS4B mediates HCV RNA replication. *J. Virol.* **78:** 11288–11295.
51. Park, C. Y., H. J. Jun, T. Wakita, J. H. Cheong, and S. B. Hwang. 2009. Hepatitis C virus nonstructural 4B protein modulates sterol regulatory element-binding protein signaling via the AKT pathway. *J. Biol. Chem.* **284:** 9237–9246.

Research Article

EASL EUROPEAN ASSOCIATION FOR THE STUDY OF THE LIVER | JOURNAL OF HEPATOLOGY

Hepatitis C virus NS4B blocks the interaction of STING and TBK1 to evade host innate immunity

Qiang Ding[1,†], Xuezhi Cao[1,†], Jie Lu[1], Bing Huang[1], Yong-Jun Liu[1,2], Nobuyuki Kato[3], Hong-Bing Shu[4], Jin Zhong[1,*]

[1]*Key Laboratory of Molecular Virology and Immunology, Institut Pasteur of Shanghai, Shanghai Institutes for Biological Sciences, Chinese Academy of Sciences, Shanghai 200025, China;* [2]*Baylor Institute for Immunology Research, 3434 Live Oak, Dallas, TX 75204, USA;* [3]*Department of Tumor Virology, Okayama University Graduate School of Medicine, Dentistry, and Pharmaceutical Sciences, Okayama 700-8558, Japan;* [4]*College of Life Sciences, Wuhan University, Wuhan, Hubei 430072, China*

Background & Aims: Hepatitis C virus (HCV) is a major human viral pathogen that causes chronic hepatitis, liver cirrhosis, and hepatocellular carcinoma. In most cases, acute HCV infection becomes persistent, at least in part due to viral evasion of host innate immune response. Although HCV genomic RNA contains pathogen-associated molecular pattern (PAMP) that is able to induce host interferon responses, HCV can shut down the responses by using the viral NS3/4A protease to cleave MAVS/VISA and TRIF, two key adaptor molecules essential for the interferon signaling activation. The aim of this study was to explore a novel NS3/4A-independent mechanism HCV utilizes to evade host innate immune responses.

Methods: We used the interferon promoter-reporter system to screen HCV encoded proteins for their activities to suppress the interferon signaling and to determine the molecular targets of viral proteins. Co-immunoprecipitation, confocal microscopy, and siRNA-based gene silencing were used to investigate the molecular mechanism.

Results: We found that, in addition to NS3/4A, NS4B can suppress double-stranded RNA or RNA virus induced interferon activation. NS4B interacts with STING/MITA, an important molecule that mediates the HCV PAMP induced interferon signaling. Mechanistic studies indicated that NS4B disrupts the interactions between STING/MITA and TBK1.

Conclusions: In conclusion, we reported an additional mechanism for HCV evasion of host interferon responses in which viral NS4B protein targets STING/MITA to suppress the interferon signaling. Our results present important evidence for the control of interferon response by HCV, and shed more light on the molecular mechanisms underlying the persistence of HCV infection.

Keywords: Hepatitis C virus; Interferon; NS4B; STING/MITA; TBK-1.

Received 1 November 2012; received in revised form 3 March 2013; accepted 11 March 2013; available online 28 March 2013

* Corresponding author. Address: Institut Pasteur of Shanghai, Chinese Academy of Sciences, 225 South Chongqing Road, Shanghai 200025, China. Tel.: +86 21 63858685; fax: +86 21 63859365.

E-mail address: jzhong@sibs.ac.cn (J. Zhong).

† These authors contributed equally to this work.

Abbreviations: HCV, hepatitis C virus; PAMP, pathogen-associated molecular pattern; STING, stimulator of interferon genes; MITA, mediator of IRF3 activation; SeV, Sendai virus; ER, endoplasmic reticulum.

Introduction

Hepatitis C virus (HCV), an enveloped, single-stranded, positive-sense RNA virus, infects 170 million people in the world, and approximately 80% of the infected individuals develop persistent infection, which leads to severe liver diseases, such as liver cirrhosis and hepatocellular carcinoma [1]. Despite a small RNA genome of 9.6-kb encoding only 10 viral structural and non-structural proteins, HCV develops multiple mechanisms to defeat host immune surveillance and responses [2], including evasion of both innate and adaptive immune responses. How HCV induces and regulates host interferon response, the first line of antiviral immune response, has been a subject of extensive research in the past years.

Virus infection can be sensed in host cells through the interaction of pathogen-associated molecular pattern (PAMP) with host pattern recognition receptors (PRRs) [3–5]. HCV genomic RNA possesses a PAMP located at its 3′ untranslated region (UTR) which consists of a poly (U/C) tract [6]. It can be recognized by retinoic acid-induced gene I (RIG-I) [3], which contains tandem N-terminal caspase recruitment domains (CARDs) that interact with another CARD domain containing protein, mitochondrial antiviral signaling (MAVS; also known as VISA, IPS-1, and Cardif) [7–10]. This interaction activates the downstream IKK/TANK-binding kinase 1 (TBK-1), the IKKαβ/γ complex as well as MAPK, leading to activation of interferon regulatory factor 3 (IRF3), IRF7, NF-κB, and AP-1. The activated transcription factors translocate to the nucleus and activate the transcription of both type I and III interferons. Recent studies have identified a new molecule, stimulator of interferon genes (STING), also named MITA (for mediator of IRF3 activation) that is critical for effective innate immune signaling responding to double-stranded DNA

transfection, bacteria and RNA virus infection [11–15]. STING/MITA predominantly resides in the endoplasmic reticulum and is able to activate both NF-κB and IRF3 transcription pathways, to induce expression of type I interferon, and exert a potent anti-viral state following expression [11,13,14]. It has been proposed that STING/MITA may undergo polymerization upon stimulation. The formed STING/MITA polymer provides a platform to bring TBK1 and IRF3 into proximity, so that phosphorylation of IRF3 by TBK1 can occur [13,16].

Viruses also evolve multiple mechanisms to fight the host interferon responses. HCV NS3/4A protease, essential for maturation of the viral polyprotein [17], can cleave the key adaptor proteins MAVS/VISA [9,18] and TRIF [19] that transmit signals from the upstream sensor molecules RIG-I and TLR3, respectively, therefore blocking both RIG-I- and TLR3-mediated activation of interferon. A detailed analysis shows that NS3/4A serine protease cleaves MAVS/VISA at Cys-508, resulting in the release of the N-terminal fragment of MAVS/VISA from the mitochondria, thus impairing the function of MAVS/VISA [9,18]. Previous studies showed that HCV may possess an NS3/4A-independent mechanism to suppress the interferon signaling [20]. The aim of this study was to explore a novel NS3/4A-independent mechanism HCV utilizes to evade host innate immune responses. We found that HCV encoded NS4B protein targets STING/MITA to prevent the interaction between STING/MITA and TBK1 upon stimulation, leading to blockade of interferon signaling.

Materials and methods

Cell culture and reagents

HEK293 and HuH7 cells were maintained in Dulbecco's modified Eagle's medium (DMEM) (Invitrogen, Carlsbad, CA, USA) supplemented with 10% fetal bovine serum (FBS), 2 mM L-glutamine, 100 U/ml penicillin, and 100 mg/ml streptomycin. PH5CH8 cells [21] were maintained in DMEM/F12 (Invitrogen) (1:1) with glutamine (2 mM, Invitrogen), epidermoid growth factor (100 ng/ml, Toyobo, Osaka, Japan), insulin (10 μg/ml, Sigma-Aldrich, St. Louis, MO, USA), linoleic acid (5 μg/ml, Sigma-Aldrich), hydrocortisone (10^{-6} M, Sigma-Aldrich), selenium (10^{-7} M, Sigma-Aldrich), transferrin (5 μg/ml, Sigma-Aldrich), prolactin (100 ng/ml, Sigma-Aldrich), and 2% fetal bovine serum. All the cells were cultured in humidified air containing 5% CO_2 at 37 °C.

Antibodies against Flag (M2; F3165) and β-actin were purchased from Sigma. Anti-HA and Myc antibodies were from Santa Cruz Biotechnology. The antibody against STING/MITA was described as previously [13] and anti-NS4B antibody was a gift from Dr. M. Kohara (Tokyo Metropolitan Institute of Medical Science) [22].

Plasmids construction

IL28 promoter reporter plasmid was previously described [23]. To construct the *IL29* promoter reporter plasmid, a 1003-bp sequence upstream of the translation start codon was amplified from cDNA of A549 cells using primers *IL29*pF(-1003) (5′-TAGGTACCGGGACATTCTTAAACCAATGGC-3′) and *IL29*pR (5′-GCAGATCTGGCTAAATCGCAACTGCTTCC-3′) in which KpnI and BglII sites were introduced, respectively. The PCR product was then cloned into pGL3-enhancer vector (Promega, Madison, WI, USA). Flag-tagged NS4B from different HCV genotypes were cloned into pcDNA3.1 to generate the NS4B expression constructs.

Flag-MAVS (C508R) mutant was generated by Quikchange (Stratagene, Santa Clara, CA, USA) site-directed mutagenesis. All the constructs were checked by DNA sequencing.

RNA isolation and quantitative RT-PCR (RT-qPCR)

Total RNA was isolated using guanidine thiocyanate (GTC) method as previously described [24]. cDNA was generated using random hexamers and TaqMan® Reverse Transcription Reagents (Applied Biosystems, Roche, NJ, USA) and amplified using SYBR® Green Real time PCR Master Mix (TOYOBO). The sequences of primers for *GAPDH*, *IFN-β*, and *IFN-λ1* were described previously [23]. For the data analysis, the Ct (threshold cycle) values for the gene of interest were normalized to those for *GAPDH*.

Co-immunoprecipitation and immunoblot analysis

HEK293 or PH5CH8 cells were transfected with various combinations of plasmids for 24 or 48 h using X-TremeGENE HP DNA Transfection Reagent (Roche, Basel, Switzerland) following the manufacturer's instructions, and then lysed in 1 ml of lysis buffer (15 mM Tris, 120 mM NaCl, 2 mM EDTA, 0.5% Triton X-100, 10 μg/ml aprotinin, 10 μg/ml leupeptin, and 0.5 mM phenylmethylsulfonyl fluoride, pH 7.5). For each immunoprecipitation, a 1-ml aliquot of lysate was incubated with 0.5 μg of the indicated monoclonal antibody and 20 μl of 1:1 slurry of GammaBind G Plus-Sepharose (Amersham Biosciences, Piscataway, NJ, USA) for 2 h. The Sepharose beads were washed three times with 1 ml of lysis buffer and 500 mM NaCl. The precipitates were fractionated by SDS–PAGE, and subsequent Western blot analysis was performed.

STING/MITA knockdown

The RNAi plasmids targeting human *STING/MITA* mRNA were as described before [13]. 1 μg of siRNA plasmids was transfected into PH5CH8 cells seeded in 12-well plates. 12 h later, 3 μg/ml puromycin was supplemented into the culture medium for 24 h. After puromycin selection, cells were used for further experiments.

Confocal microscopy

To determine the NS4B and STING/MITA co-localization, HuH7 or PH5CH8 cells were grown on the coverslips for 24 h prior to the transfection of Flag-NS4B and STING-Myc. At 24 or 48 h post-transfection, the cells were washed with phosphate-buffered saline (PBS), fixed with ice-cold ethanol, blocked, and then permeabilized in PBS containing 5% FBS and 0.05% Tween-20, and incubated with mouse anti-Flag (Sigma) and rabbit anti-Myc (Sigma). After washing with PBS, cells were incubated with Alexa FluorR 488 goat anti-mouse secondary antibody and Alexa FluorR 555 goat anti-rabbit secondary antibody (Invitrogen).

To examine the co-localization of STING/MITA and NS4B in the context of HCV infection, HuH7 cells were transfected with the STING-Myc expression plasmid for 24 h prior to HCVcc (JFH1) infection at a multiplicity of infection of 1. At 48 h post-infection, the cells were fixed and processed as described above. The cells were visualized under a fluorescent microscope and images were captured with Zeiss AxioCam MRm camera.

Luciferase reporter assay

One hundred thousand HEK293 cells were seeded into 48-well plates overnight prior to transfection with 50 ng/well of the indicated *IL28*-Luc, *IL29*-Luc or *IFN-β*-Luc constructs; 50 ng/well of CMV promoter driven *Renilla* luciferase vector (pRL-CMV; Promega) was included for normalization of transfection efficiency. One day after plasmid transfection, the cells were inoculated with Sendai virus (SeV, 10HAU/ml) and harvested at 8 h post-infection. Cell lysates were assayed for luciferase activities using the Dual-Luciferase Reporter Assay System (Promega) following the manufacturer's instructions.

Results

HCV NS4B blocks type I and type III interferon induction

Our previous results showed that HCV-encoded NS3/4A protease can suppress type III interferon induction [23]. It was demonstrated that HCV may possess an NS3/4A-independent mechanism to suppress type I interferon induction [20]. To explore this potential mechanism, we first determined whether SeV-triggered IFN-β activation was affected by other HCV-encoded proteins besides the NS3/4A protease. The plasmids encoding structural or non-structural proteins of the HCV JFH1 strain were co-transfected with IFN-β reporter plasmid into HEK293 cells followed by SeV infection, and luciferase activity was measured. We

found that both NS3/4A and NS4B could inhibit SeV induced IFN-β activation while other HCV proteins did not have a significant impact (data not shown). To confirm this observation, we transfected HEK293 cells with plasmids expressing NS3/4A or NS4B, together with a plasmid expressing firefly luciferase reporter driven by the *IFN-β* [25], *IL28* (IFN-λ2/3) [23] or *IL29* (IFN-λ1) promoters, and a plasmid expressing *Renilla* luciferase serving as the transfection control. After SeV stimulation, the interferon promoter-driven luciferase activities were measured. We found that both NS4B and NS3/4A suppressed the SeV induced IFN-β and IFN-λ activation (Fig. 1A–C). Altogether, our data indicate that NS4B suppresses RNA virus induced type I and type III interferon production.

Next, we tested the effects of NS4B of different HCV strains on interferon activation. Plasmids expressing NS4B of HCV strain J6 (genotype 2a), con1 (genotype 1b) and JFH1 (genotype 2a), and the IFN-β reporter plasmid were transfected into HEK293 cells followed by SeV stimulation. We found that NS4B of all tested HCV strains displayed an inhibitory effect on IFN-β induction (Supplementary Fig. 1).

NS4B inhibits interferon induction at a step upstream of IRF3 and NF-κB

To determine the molecular target of NS4B in the interferon induction signaling pathway, we transfected the plasmid expressing NS4B and plasmids expressing a molecule in the RIG-I signaling pathway, such as RIG-IN, MAVS/VISA, IKK-ε, TBK-1, STING/MITA, IRF3 or NF-κB p65, into HEK293 cells together with the IFN-β reporter plasmid. Luciferase assays were performed 24 h after transfection. Interestingly, NS4B inhibited the induction of IFN-β by RIG-IN, MAVS/VISA, IKK-ε, TBK-1, and STING/MITA. In contrast, the induction of IFN-β by IRF3 and p65 was not affected by NS4B (Fig. 1 D-H), suggesting that NS4B likely inhibits the interferon signaling pathway at a step upstream of IRF3 and NF-κB p65.

NS4B interacts with STING/MITA

Recent studies have suggested that STING/MITA functions as a scaffold protein to promote the phosphorylation of IRF3 by TBK-1 [16]. In addition, it was shown that the NS4B protein of yellow fever virus could interact with STING/MITA and blocked the interferon induction [12]. Therefore, we hypothesized that HCV NS4B may also target STING/MITA to block interferon signaling.

To probe the molecular interactions of NS4B and STING/MITA, we co-transfected the plasmids expressing Flag-tagged NS4B and Myc-tagged STING into HEK293 cells, and the Myc-tagged MAVS/VISA was included in parallel as a control. As shown in Fig. 2A, the anti-Flag antibody could efficiently precipitate STING/MITA but not MAVS/VISA, indicating that NS4B interacts with STING/MITA. Next, we determined the interactions of NS4B and STING/MITA in hepatocytes. To do so, we first checked the STING/MITA protein expression levels in various hepatic cell lines. As shown in Fig. 2B, STING/MITA was expressed at a high level in PH5CH8 and HepG2 hepatic cells as well as in HEK293 cells, but was barely expressed in HuH7 hepatic cells, the sole cell line supporting HCV infection. Therefore, next we examined whether NS4B interacts with endogenous STING/MITA in PH5CH8 hepatocytes. Plasmids expressing Flag-tagged NS4B or NS5A (negative control)

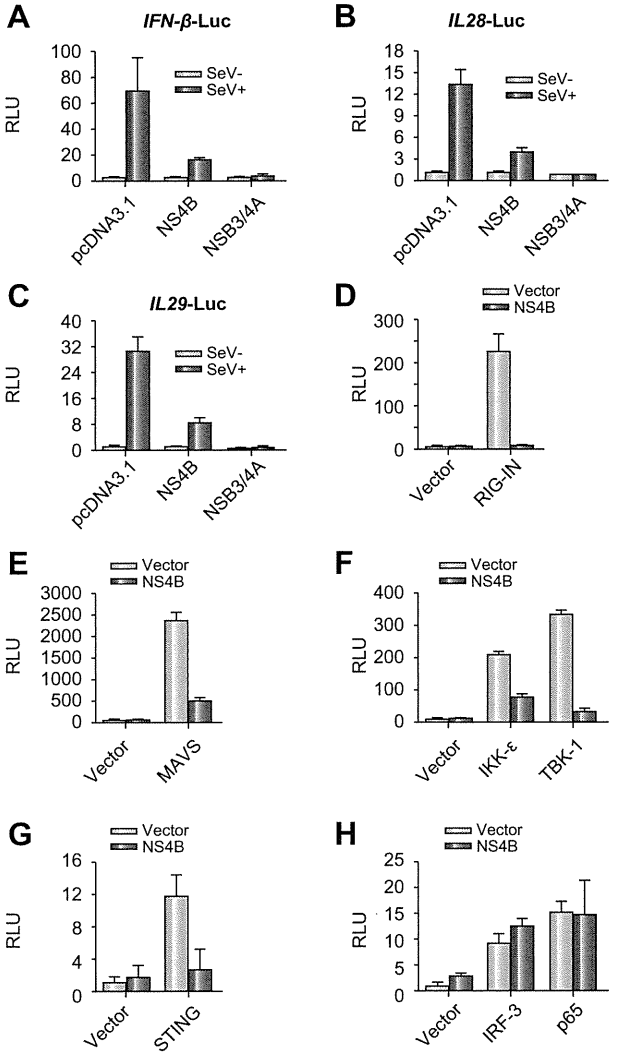

Fig. 1. HCV NS4B blocks interferon induction at a step upstream of IRF3 and NF-κB. (A–C) HEK293 cells were co-transfected with the interferon reporter plasmids, such as *IFN-β*-Luc (A), *IL28*-Luc (B) or *IL29*-Luc (C) together with the plasmids expressing HCV NS3/4A or NS4B, followed by SeV inoculation. Luciferase activities were determined 8 h post-infection. (D–H) HEK293 cells were co-transfected with the *IFN-β*-Luc reporter plasmid, NS4B expressing plasmid, together with a plasmid expressing RIG-IN (D), MAVS/VISA (E), TBK1, IKK-ε (F), STING/MITA (G), IRF3-5D or NF-κB p65 (H). Luciferase activities were measured 24 h after transfection, and the results are presented as fold induction of *IFN-β* promoter activity. Error bars represent standard deviations of triplicates.

were transfected into PH5CH8 cells, and immunoprecipitation was performed using an anti-Flag antibody. As shown in Fig. 2C, endogenous STING/MITA can be co-immunoprecipitated with NS4B but not with NS5A, indicating that NS4B interacts with endogenous STING/MITA. This result was also confirmed by confocal analysis, showing that NS4B colocalizes with endogenous STING/MITA in PH5CH8 cells, with both proteins showing the previously reported endoplasmic reticulum (ER) membrane localization pattern [11,14] (Fig. 2D). Finally, to examine the NS4B-STING/MITA interaction in the context of HCV infection, we transfected HuH7 cells with Myc-tagged STING and then infected the cells with HCVcc. Confocal microscopic analysis

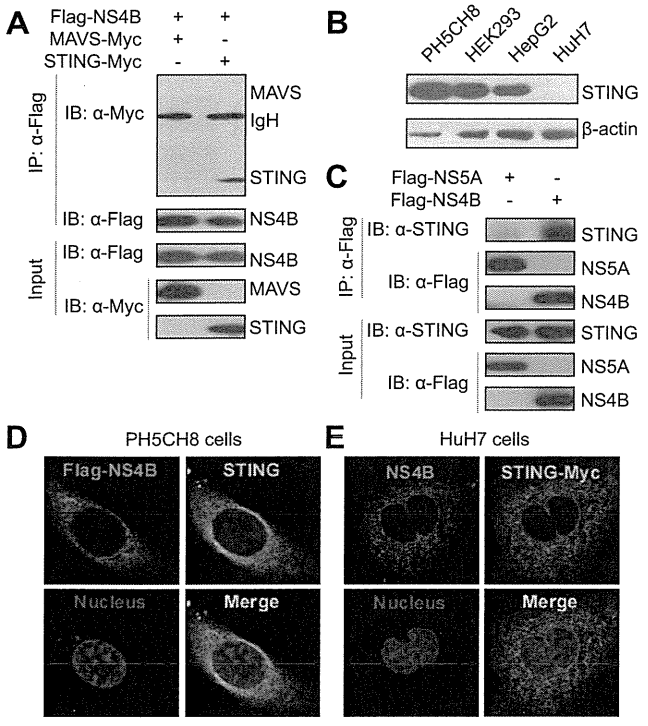

Fig. 2. HCV NS4B interacts with STING/MITA. (A) HEK293 cells were transfected with plasmids expressing Flag-NS4B and STING-Myc or MAVS-Myc. Cell lysates were immunoprecipitated with an anti-Flag antibody 24 h post-transfection. The immunoprecipitates were analyzed by immunoblotting with an anti-Myc antibody (top). The expression of NS4B, STING/MITA and MAVS/VISA was analyzed by immunoblotting with anti-Myc and anti-Flag antibodies (middle and bottom), respectively; (B) measurement of endogenous STING/MITA protein expression in various cell lines by Western blotting analysis using the anti-human STING/MITA antibody. (C) PH5CH8 cells were transfected with plasmids expressing Flag-NS4B or Flag-NS5A. Cell lysates were immunoprecipitated with anti-Flag antibody and analyzed by immunoblotting with anti-STING antibody (top). The expression of the input proteins was analyzed by immunoblotting with anti-Flag and anti-STING antibodies (middle and bottom), respectively. (D) PH5CH8 cells were transfected with the plasmid expressing Flag-NS4B, and then stained with anti-Flag and anti-STING antibodies. Nuclei were stained with DAPI. (E) HuH7 cells transfected with STING-Myc were infected with JFH1-HCVcc at an MOI of 1 for 48 h, and then stained with anti-NS4B and anti-Myc antibodies. The experiments were repeated for three times with similar results.

showed that NS4B and STING/MITA indeed colocalize (Fig. 2E). Collectively, these results indicate that STING/MITA and NS4B interact with each other.

NS4B disrupts the interaction between STING/MITA and TBK1

To probe how the NS4B-STING interaction affects STING/MITA biological function, we first examined whether NS4B had any effect on endogenous STING/MITA protein levels. Increasing amounts of plasmids expressing NS4B were transfected into PH5CH8 cells, and endogenous STING/MITA protein levels were determined by Western blot. As shown in Fig. 3A, the endogenous STING/MITA protein levels were not affected by NS4B.

It was shown that oligomerization of STING/MITA is essential for mediating the interferon signaling pathway [13,16], we thus examined whether NS4B impaired the STING/MITA oligomerization. The plasmids expressing the HA- and Flag-tagged STING/MITA were co-transfected together with Flag-NS4B into PH5CH8 cells, and the cell lysates were immunoprecipitated with an anti-HA antibody and probed with an anti-Flag antibody. As shown in Fig. 3B, the STING/MITA oligomerization was not affected by NS4B.

Next, we examined whether NS4B impaired the interaction between STING/MITA and MAVS/VISA. The plasmids expressing HA-tagged MAVS, Flag-tagged NS4B, and Flag-tagged STING were co-transfected into PH5CH8 cells, and the cell lysates were immunoprecipitated with an anti-HA antibody and probed with an anti-Flag antibody. Fig. 3C shows that STING/MITA could be co-immunoprecipitated by the anti-HA (MAVS) antibody, and this interaction was not affected by NS4B.

Furthermore, we examined whether NS4B impairs the interaction between STING/MITA and TBK1, the important step for transducing the interferon signaling [11,13,16]. Plasmids expressing Flag-tagged STING and HA-tagged TBK1 were co-transfected together with Flag-NS4B into PH5CH8 cells, and the cell lysates were immunoprecipitated with an anti-HA antibody and probed with an anti-Flag antibody. As shown in Fig. 3D, NS4B dramatically impaired the STING/MITA-TBK-1 interaction.

We also performed these assays in HEK293 cells, and found that NS4B impaired the interaction of STING/MITA and TBK1 while had no effect on the oligomerization of STING/MITA and the interaction between STING/MITA and MAVS/VISA (Supplementary Fig. 2).

STING/MITA is important for HCV PAMP-induced interferon activation

It has been proposed that STING/MITA plays an important role in interferon response induced by bacteria infection or dsDNA. The finding that NS4B could target STING/MITA to block the interferon signaling raised the question as to whether STING/MITA is important for HCV PAMP induced interferon responses. To address this question, we transfected two sets of *STING/MITA*-specific siRNA to knockdown STING/MITA expression in PH8CH5 cells. As shown in Fig. 4A–C, knockdown of STING/MITA significantly decreased HCV 3'UTR induced endogenous *IFN-β* and *IFN-λ* mRNA levels, suggesting that STING/MITA is important for HCV PAMP triggered type I and III interferon activation.

To further demonstrate that NS4B blocks the interferon signaling in a manner independent of MAVS/VISA cleavage by the NS3/4A protease, we co-transfected plasmids expressing NS4B or NS3/4A, plasmids expressing the wild type or NS3/4A protease insensitive mutant (C508R) MAVS/VISA [18], together with the IFN-β reporter plasmids into PH5CH8 cells. As shown in Fig. 4D, NS3/4A could efficiently block the interferon signaling mediated by the wild type MAVS/VISA, but not by the C508R mutant MAVS/VISA, whereas NS4B could equally block the interferon signaling mediated by both wild type and C508 mutant MAVS/VISA, albeit with a lower efficiency than NS3/4A. These results suggest that NS3/4A and NS4B may synergistically inhibit different steps of interferon signaling during HCV infection.

Discussion

It is well recognized that HCV encoded NS3/4A protease cleaves MAVS/VISA and TRIF to shut down the interferon signaling mediated by RIG-I and TLR3, respectively. Here we demonstrate that HCV possesses an additional mechanism to contribute to the

Research Article

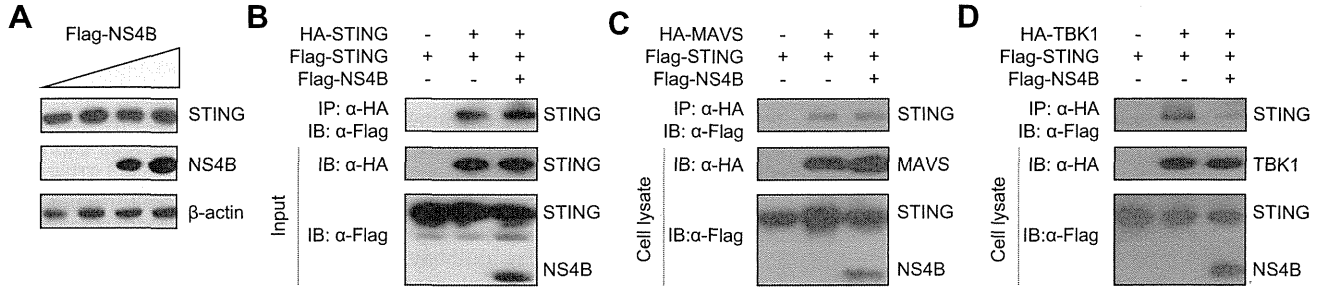

Fig. 3. NS4B disrupts the interaction between STING/MITA and TBK1. (A) PH5CH8 cells were transfected with an increasing amount of plasmids expressing Flag-NS4B (0, 0.2, 0.6, and 1 μg), and cell lysates were analyzed by immunoblotting with anti-Flag or anti-STING antibodies at 48 h post-transfection. (B-D) PH5CH8 cells were transfected with plasmids expressing Flag-STING, Flag-NS4B together with either HA-STING (B), or HA-MAVS (C), or HA-TBK1 (D). Cell lysates were immunoprecipitated with the anti-HA antibody at 48 h post-transfection. The immunoprecipitates were analyzed by immunoblotting with anti-Flag antibody (top). The expression of the input proteins was analyzed by immunoblotting with the anti-HA and anti-Flag antibodies (middle and bottom), respectively. The experiments were repeated three times with similar results.

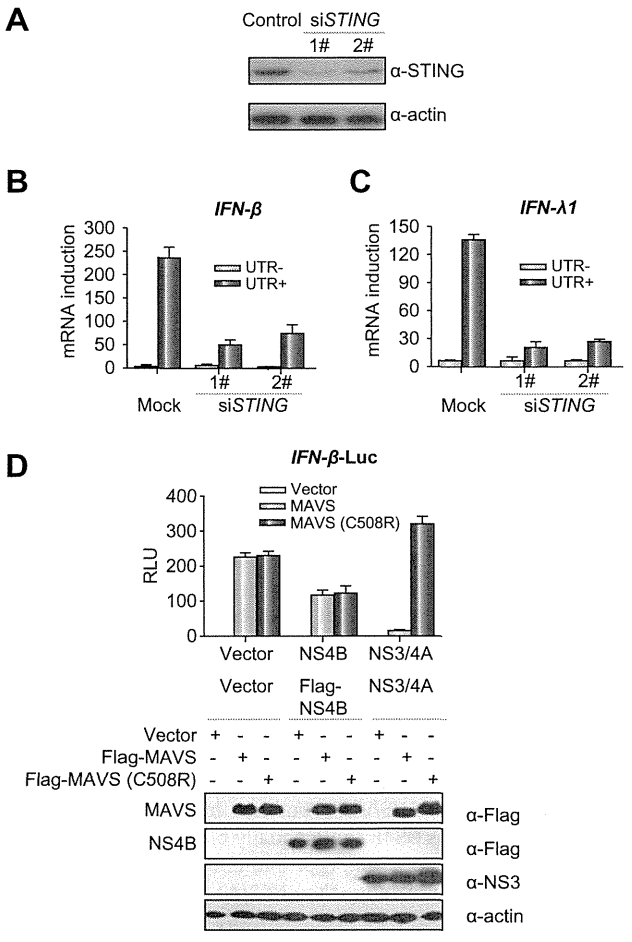

Fig. 4. STING/MITA is required for the HCV PAMP-induced interferon signaling. (A–C) Two sets of siRNAs targeting human *STING/MITA* were transfected into PH5CH8 cells. Twenty-four hours post-transfection, cells were transfected again with HCV 3′ UTR RNA for 16 h, and then *IFN-β* (B) or *IFN-λ* (C) mRNA levels were determined by RT-qPCR analysis. The STING/MITA knockdown efficiency in PH5CH8 cells was analyzed by immunoblotting (A). (D) PH5CH8 cells were co-transfected with *IFN-β*-Luc together with the plasmids expressing Flag-MAVS or Flag-MAVS (C508R) and plasmids expressing NS3/4A or NS4B. Luciferase activities were determined at 24 h post-transfection. The expression of the proteins was analyzed by immunoblotting with the anti-Flag, anti-NS3 or anti-actin antibodies, respectively. Error bars represent standard deviations of triplicates.

evasion of innate immune response. NS4B protein interacts with STING/MITA to impair the interaction between STING/MITA and TBK1, thereby suppressing the interferon signaling. Although NS3/4A suppresses the interferon signaling very efficiently especially in the *in vitro* experiments, mostly involving overexpression of NS3/4A proteins in cell lines, there are several reasons why HCV needs multiple mechanisms to ensure silencing of antiviral interferon signaling upon infection. First, there could be incomplete cleavage of MAVS/VISA and TRIF due to the lower expression of NS3/4A protease in the context of HCV infection *in vivo*. NS4B could be in place to block these signals that are transmitted through uncleaved MAVS/VISA and TRIF. Second, NS4B could block the MAVS/VISA independent interferon signaling triggered by HCV infection. Indeed, a recent report suggests that STING/MITA is required for the virus-host cell fusion triggered interferon signaling activation that may also require TLR7 and TLR9 [26]. As an envelope virus, HCV entry involves the fusion of viral envelope and host cell membranes. It will be interesting to investigate whether HCV entry could trigger interferon signaling, whether STING/MITA is required for this response, and whether NS4B can block this response. Recent studies have reported that several flaviviruses, including yellow fever virus [12] and dengue virus [27,28], can target STING/MITA to suppress the interferon signaling by various mechanisms. NS4B of yellow fever virus can interact with STING/MITA to block the RIG-I mediated interferon signaling, while dengue virus encodes a protease NS2B3 to cleave STING/MITA to shut down the signaling. These studies provide evidence to support the critical roles of STING/MITA in innate immune response to RNA virus infection, and also highlight the significance of targeting STING/MITA to escape innate immunity for the benefit of virus survival.

While we were finishing up the manuscript, Nitta *et al.* [29] reported that NS4B binds to STING/MITA and shuts down the interferon signaling. Nevertheless, there are critical differences in the mechanisms between these two studies. Nitta *et al.* showed that NS4B impairs the interactions between STING/MITA and MAVS/VISA, while our results indicate that NS4B does not have any effect on the interactions between STING/MITA and MAVS/VISA, but instead impairs the interaction of STING/MITA and TBK1. Because Nitta *et al.* did not examine the effect of NS4B on the interaction of STING/MITA and TBK1, so it is not known whether the inhibition of STING/MITA and TBK1 interaction can be also found in their study. It was recently reported that

MAVS/VISA mainly resides on mitochondrial-associated endoplasmic reticulum membrane (MAM), which is a dynamic structure serving as a major site for assembling a complex with RIG-I to transmit the interferon signaling [30]. It was not clear whether STING/MITA is a part of this complex on MAM. The discrepancy in the effect of NS4B on STING and MAVS interaction between Nitta *et al.* and our study may due to the dynamic changes of MAM structures upon virus infection.

Tanaka and Chen [16] used an *in vitro* reconstitution system to shows that upon stimulation, STING/MITA forms a polymer to provide a scaffold to assemble IRF3 and TBK1, which leads to TBK1-dependent phosphorylation of IRF3. Our finding that HCV NS4B protein prevents the interaction between TBK1 and STING/MITA to block the interferon signaling fits well this model, and is also consistent with our results that NS4B inhibits the interferon signaling induced by the overexpression of TBK1 and STING/MITA (Fig. 1). Saitoh *et al.* reported that upon stimulation, the ER localized STING/MITA can translocate to the cytoplasmic punctate structures to assemble with TBK1, and this translocation is essential for the innate immune response [31]. The ER localized HCV NS4B protein may retain STING/MITA at the ER to inhibit the interaction of STING/MITA with TBK1.

In conclusion, we reported an additional mechanism for HCV evasion of host interferon responses in which viral NS4B protein targets STING/MITA to suppress the interferon signaling. Our results presented important evidence for the control of interferon response by HCV, and shed more light on the molecular mechanisms underlying the persistence of HCV infection.

Financial support

This work was supported by grants from the Chinese National Science and Technology Major Project (2012ZX10002007-003), the Chinese MOST 973 Program (2009CB522501; 2009CB522504), the CAS/SAFEA International Partnership Program for Creative Research Teams, and Institut Pasteur International Network (ACIP-AP20, 2010).

Conflict of interest

The authors who have taken part in this study declared that they do not have anything to disclose regarding funding or conflict of interest with respect to this manuscript.

Acknowledgements

We thank Dr. M. Kohara (The Tokyo Metropolitan Institute of Medical Science, Tokyo, Japan) for the NS4B antibody. We also thank Caoqi Lei, Xi Kang and Jing Zhang (Wuhan University, Wuhan, China) for technical assistance.

Supplementary data

Supplementary data associated with this article can be found, in the online version, at http://dx.doi.org/10.1016/j.jhep.2013.03.019.

References

[1] Singh GK, Hoyert DL. Social epidemiology of chronic liver disease and cirrhosis mortality in the United States, 1935–1997: trends and differentials by ethnicity, socioeconomic status, and alcohol consumption. Hum Biol 2000;72:801–820.
[2] Dustin LB, Rice CM. Flying under the radar: the immunobiology of hepatitis C. Annu Rev Immunol 2007;25:71–99.
[3] Yoneyama M, Kikuchi M, Natsukawa T, Shinobu N, Imaizumi T, Miyagishi M, et al. The RNA helicase RIG-I has an essential function in double-stranded RNA-induced innate antiviral responses. Nat Immunol 2004;5:730–737.
[4] Akira S, Takeda K. Toll-like receptor signalling. Nat Rev Immunol 2004;4:499–511.
[5] Honda K, Taniguchi T. IRFs: master regulators of signalling by Toll-like receptors and cytosolic pattern-recognition receptors. Nat Rev Immunol 2006;6:644–658.
[6] Saito T, Owen DM, Jiang F, Marcotrigiano J, Gale Jr M. Innate immunity induced by composition-dependent RIG-I recognition of hepatitis C virus RNA. Nature 2008;454:523–527.
[7] Xu LG, Wang YY, Han KJ, Li LY, Zhai Z, Shu HB. VISA is an adapter protein required for virus-triggered IFN-beta signaling. Mol Cell 2005;19:727–740.
[8] Seth RB, Sun L, Ea CK, Chen ZJ. Identification and characterization of MAVS, a mitochondrial antiviral signaling protein that activates NF-kappaB and IRF 3. Cell 2005;122:669–682.
[9] Meylan E, Curran J, Hofmann K, Moradpour D, Binder M, Bartenschlager R, et al. Cardif is an adaptor protein in the RIG-I antiviral pathway and is targeted by hepatitis C virus. Nature 2005;437:1167–1172.
[10] Kawai T, Takahashi K, Sato S, Coban C, Kumar H, Kato H, et al. IPS-1, an adaptor triggering RIG-I- and Mda5-mediated type I interferon induction. Nat Immunol 2005;6:981–988.
[11] Sun W, Li Y, Chen L, Chen H, You F, Zhou X, et al. ERIS, an endoplasmic reticulum IFN stimulator, activates innate immune signaling through dimerization. Proceedings of the National Academy of Sciences 2009;106:8653–8658.
[12] Ishikawa H, Ma Z, Barber GN. STING regulates intracellular DNA-mediated, type I interferon-dependent innate immunity. Nature 2009;461:788–792.
[13] Zhong B, Yang Y, Li S, Wang Y-Y, Li Y, Diao F, et al. The adaptor protein MITA links virus-sensing receptors to IRF3 transcription factor activation. Immunity 2008;29:538–550.
[14] Ishikawa H, Barber GN. STING is an endoplasmic reticulum adaptor that facilitates innate immune signalling. Nature 2008;455:674–678.
[15] Burdette DL, Monroe KM, Sotelo-Troha K, Iwig JS, Eckert B, Hyodo M, et al. STING is a direct innate immune sensor of cyclic di-GMP. Nature 2011;478:515–518.
[16] Tanaka Y, Chen ZJ. STING specifies IRF3 phosphorylation by TBK1 in the cytosolic DNA signaling pathway. Sci Signal 2012;5:ra20.
[17] Bartenschlager R, Ahlborn-Laake L, Mous J, Jacobsen H. Nonstructural protein 3 of the hepatitis C virus encodes a serine-type proteinase required for cleavage at the NS3/4 and NS4/5 junctions. J Virol 1993;67:3835–3844.
[18] Li XD, Sun L, Seth RB, Pineda G, Chen ZJ. Hepatitis C virus protease NS3/4A cleaves mitochondrial antiviral signaling protein off the mitochondria to evade innate immunity. Proc Natl Acad Sci U S A 2005;102:17717–17722.
[19] Li K, Foy E, Ferreon JC, Nakamura M, Ferreon AC, Ikeda M, et al. Immune evasion by hepatitis C virus NS3/4A protease-mediated cleavage of the Toll-like receptor 3 adaptor protein TRIF. Proc Natl Acad Sci U S A 2005;102:2992–2997.
[20] Cheng G, Zhong J, Chisari FV. Inhibition of dsRNA-induced signaling in hepatitis C virus-infected cells by NS3 protease-dependent and -independent mechanisms. Proc Natl Acad Sci U S A 2006;103:8499–8504.
[21] Naganuma A, Dansako H, Nakamura T, Nozaki A, Kato N. Promotion of microsatellite instability by hepatitis C virus core protein in human non-neoplastic hepatocyte cells. Cancer Res 2004;64:1307–1314.
[22] Hügle T, Fehrmann F, Bieck E, Kohara M, Kräusslich H-G, Rice CM, et al. The hepatitis C virus nonstructural protein 4B is an integral endoplasmic reticulum membrane protein. Virology 2001;284:70–81.
[23] Ding Q, Huang B, Lu J, Liu Y-J, Zhong J. Hepatitis C virus NS3/4A protease blocks IL-28 production. Eur J Immunol 2012;42:2374–2382.
[24] Chomczynski P, Sacchi N. Single-step method of RNA isolation by acid guanidinium thiocyanate-phenol-chloroform extraction. Anal Biochem 1987;162:156–159.
[25] Cheng G, Zhong J, Chung J, Chisari FV. Double-stranded DNA and double-stranded RNA induce a common antiviral signaling pathway in human cells. Proc Natl Acad Sci U S A 2007;104:9035–9040.

Research Article

[26] Holm CK, Jensen SB, Jakobsen MR, Cheshenko N, Horan KA, Moeller HB, et al. Virus-cell fusion as a trigger of innate immunity dependent on the adaptor STING. Nat Immunol 2012;13:737–743.
[27] Yu CY, Chang TH, Liang JJ, Chiang RL, Lee YL, Liao CL, et al. Dengue virus targets the adaptor protein MITA to subvert host innate immunity. PLoS Pathog 2012;8:e1002780.
[28] Aguirre S, Maestre AM, Pagni S, Patel JR, Savage T, Gutman D, et al. DENV inhibits type I IFN production in infected cells by cleaving human STING. PLoS Pathog 2012;8:e1002934.
[29] Nitta S, Sakamoto N, Nakagawa M, Kakinuma S, Mishima K, Kusano-Kitazume A, et al. Hepatitis C virus NS4B protein targets STING and abrogates RIG-I-mediated type-I interferon-dependent innate immunity. Hepatology 2013;57:46–58.
[30] Horner SM, Liu HM, Park HS, Briley J, Gale Jr M. Mitochondrial-associated endoplasmic reticulum membranes (MAM) form innate immune synapses and are targeted by hepatitis C virus. Proc Natl Acad Sci U S A 2011;108:14590–14595.
[31] Saitoh T, Fujita N, Hayashi T, Takahara K, Satoh T, Lee H, et al. Atg9a controls dsDNA-driven dynamic translocation of STING and the innate immune response. Proceedings of the National Academy of Sciences 2009;106:20842–20846.

PLOS ONE

Inhibitory Effects of Caffeic Acid Phenethyl Ester Derivatives on Replication of Hepatitis C Virus

Hui Shen[1], Atsuya Yamashita[1], Masamichi Nakakoshi[2], Hiromasa Yokoe[3], Masashi Sudo[3], Hirotake Kasai[1], Tomohisa Tanaka[1], Yuusuke Fujimoto[1], Masanori Ikeda[4], Nobuyuki Kato[4], Naoya Sakamoto[5], Hiroko Shindo[6], Shinya Maekawa[6], Nobuyuki Enomoto[6], Masayoshi Tsubuki[3]*, Kohji Moriishi[1]*

1 Department of Microbiology, Division of Medicine, Graduate School of Medicine and Engineering, University of Yamanashi, Yamanashi, Japan, **2** Faculty of Pharmaceutical Sciences, Toho University, Chiba, Japan, **3** Institute of Medical Chemistry, Hoshi University, Tokyo, Japan, **4** Department of Tumor Virology, Okayama University Graduate School of Medicine, Dentistry, and Pharmaceutical Sciences, Okayama, Japan, **5** Department of Gastroenterology and Hepatology, Hokkaido University Graduate School of Medicine, Sapporo, Japan, **6** First Department of Internal Medicine, Faculty of Medicine, University of Yamanashi, Yamanashi, Japan

Abstract

Caffeic acid phenethyl ester (CAPE) has been reported as a multifunctional compound. In this report, we tested the effect of CAPE and its derivatives on hepatitis C virus (HCV) replication in order to develop an effective anti-HCV compound. CAPE and CAPE derivatives exhibited anti-HCV activity against an HCV replicon cell line of genotype 1b with EC_{50} values in a range from 1.0 to 109.6 μM. Analyses of chemical structure and antiviral activity suggested that the length of the n-alkyl side chain and catechol moiety are responsible for the anti-HCV activity of these compounds. Caffeic acid n-octyl ester exhibited the highest anti-HCV activity among the tested derivatives with an EC_{50} value of 1.0 μM and an SI value of 63.1 by using the replicon cell line derived from genotype 1b strain Con1. Treatment with caffeic acid n-octyl ester inhibited HCV replication of genotype 2a at a similar level to that of genotype 1b irrespectively of interferon signaling. Caffeic acid n-octyl ester could synergistically enhance the anti-HCV activities of interferon-alpha 2b, daclatasvir, and VX-222, but neither telaprevir nor danoprevir. These results suggest that caffeic acid n-octyl ester is a potential candidate for novel anti-HCV chemotherapy drugs.

Citation: Shen H, Yamashita A, Nakakoshi M, Yokoe H, Sudo M, et al. (2013) Inhibitory Effects of Caffeic Acid Phenethyl Ester Derivatives on Replication of Hepatitis C Virus. PLoS ONE 8(12): e82299. doi:10.1371/journal.pone.0082299

Editor: Hak Hotta, Kobe University, Japan

Received September 15, 2013; **Accepted** October 31, 2013; **Published** December 17, 2013

Funding: This work was supported in part by grants-in-aid from the Ministry of Health, Labor, and Welfare and from the Ministry of Education, Culture, Sports, Science, and Technology of Japan. The funders had no role in study design, data collection and analysis, decision to publish, or preparation of the manuscript.

Competing Interests: The authors have declared that no competing interests exist.

* E-mail: tsubuki@hoshi.ac.jp (MT); kmoriishi@yamanashi.ac.jp (KM)

Introduction

Hepatitis C virus (HCV) is well known as a major causative agent of chronic liver disease including cirrhosis and hepatocellular carcinoma and is thought to persistently infect 170 million patients worldwide [1]. HCV belongs to the genus *Hepacivirus* of the family *Flaviviridae* and possesses a viral genome that is characterized by a single positive strand RNA with a nucleotide length of 9.6 kb [2]. The single polypeptide coded by the genome is composed of 3,000 amino acids and is cleaved by host and viral proteases, resulting in 10 proteins, which are classified into structural and nonstructural proteins [3]. The viral genome is transcribed by a replication complex consisting of NS3 to NS5B and host factors [4]. NS3 forms a complex with NS4A and becomes a fully active form to cleave the C-terminal parts of the nonstructural proteins. The advanced NS3/4A protease inhibitors, telaprevir and boceprevir, have been employed in the treatment of chronic hepatitis C patients infected with genotype 1 [5]. Sustained virologic response (SVR) was reportedly 80% in patients infected with genotype 1 following triple combination therapy with pegylated interferon, ribavirin, and telaprevir [6], although the therapy exhibits side effects including rash, severe cutaneous eruption, influenza-like symptoms, cytopenias, depression, and anemia [7]. In addition, there is the possibility of the emergence of drug-resistant viruses following treatment with those anti-HCV drugs [8] Thus, further study is required for development of safer and more effective anti-HCV compounds.

Several recent reports indicate that silbinin [9], epigallocatechin-3-gallate [10], curcumin [11], quercetin [12] and proanthocyanidins [13], which all originate from natural sources, have exhibited inhibitory activity against HCV replication in cultured cells. Caffeic acid phenethyl ester (CAPE) is an active component included in propolis prepared from honeybee hives, and has a similar structure to flavonoids (Fig. 1A). CAPE has multifunctional properties containing anti-inflammatory [14], antiviral [15], anticarcinogenic [16], and immunomodulatory activities [15]. CAPE also inhibits enzymatic activities of endogenous and viral proteins [17–19] and transcriptional activity of NF-kappaB [14,20]. In addition, CAPE could suppress HCV replication enhanced by using the NF-kappaB activation activity of morphine [21], although it has been unknown which of moieties including CAPE is responsible for anti-HCV activity. Furthermore, it is not clear whether chemical modification of CAPE could enhance anti-HCV activity or not. In this report, we examined the effect of

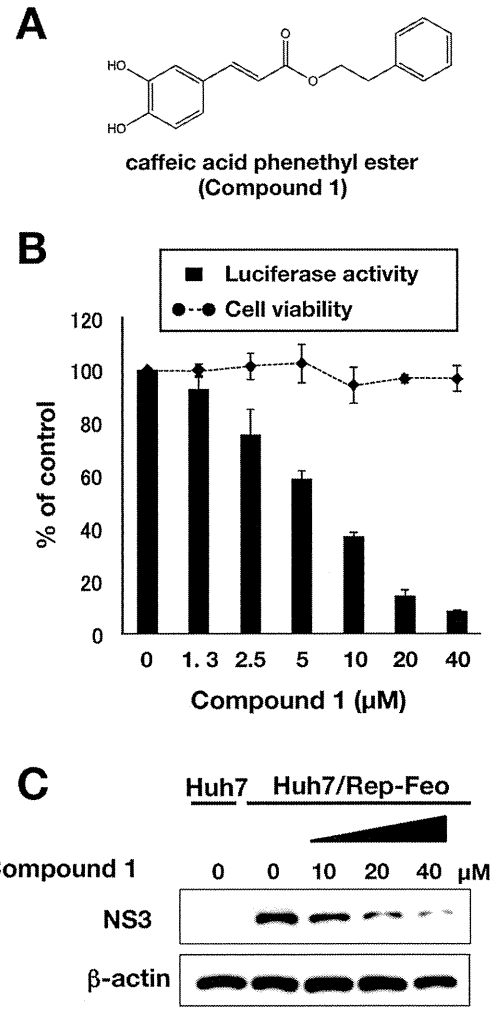

Figure 1. Effect of CAPE on viral replication in the replicon cell line of genotype 1b. (A) Molecular structure of CAPE. (B) Huh7/Rep-Feo cells were incubated for 72 h in a medium containing various concentrations of CAPE. Luciferase and cytotoxicity assays were carried out by the method described in Materials and Methods. Error bars indicate standard deviation. The data represent results from three independent experiments. (C) Protein extract was prepared from Huh7/Rep-Feo cells treated for 72 h with the indicated concentration of CAPE and it was then was subjected to Western blotting using antibodies to NS3 and beta-actin.
doi:10.1371/journal.pone.0082299.g001

CAPE derivatives on HCV proliferation to develop more effective and safer anti-HCV compounds.

Results

Effect of CAPE on HCV RNA replication in HCV subgenomic replicon cells

CAPE is composed of ester of caffeic acid and phenethyl alcohol (Fig. 1A). We examined the effect of CAPE (compound **1**) on both viral replication and cell growth in the HCV subgenomic replicon cell line Huh7/Rep-Feo. The replicon cell line was treated with various concentrations of compound **1**. The replication level of the HCV RNA was measured as an enzymatic activity of luciferase, which is bicistronically, encoded on the replicon RNA. Compound **1** suppressed HCV RNA replication at concentrations from 1.3 to 40 μM in a dose-dependent manner, but did not affect cell viability (Fig. 1B). HCV NS3, which is a viral protease, was decreased at the protein level by treatment with CAPE in a dose-dependent manner, corresponding to the viral replication, whereas beta-actin was not changed in the replicon cell line (Fig. 1C). Based on the calculation using a dose dependency of CAPE, compound **1** exhibited an EC_{50} value of 9.0 μM and a CC_{50} value of 136.1 μM, giving a selectivity index estimate (SI) of 17.9 (Table 1). These results suggest that treatment with CAPE inhibits HCV replication in HCV subgenomic replicon cells.

Structure-activity relationship of CAPE analogues

To clarify the structure-activity relationship of CAPE analogues, we examined the effect of hydroxyl groups on the aromatic ring (catechol moiety), the alkenyl moieties on alpha, beta-unsaturated esters, and the ester parts as follows (Figure S1).

We tested whether commercially available CAPE-related compounds **2** to **6** (Fig. S1) affected HCV replication (Table 1). All these compounds showed weaker inhibitory activity than CAPE (**1**), but are not toxic. Compound **2**, which is the acid component of CAPE, showed a slightly lower value of EC_{50} than compound **3**, which is the compound **2** derivative replaced a hydroxyl group with a methoxyl group of catechol moiety, while compound **4**, which is the derivative lacking two hydroxyl groups within catechol moiety, exhibits a higher value of EC_{50} than compounds **1** and **2**. These data suggest that the catechol moiety of CAPE is required for anti-HCV activity. Interestingly, compounds **5** and **6**, which are natural products including polyhydroxylated acid moieties in the ester parts, showed much weaker inhibitions than compound **1** and exhibits low *Clog P* values. The position of hydroxyl group or/and the structure of the ester part may affect the inhibitory activity and/or hydrophobicity.

We next examined the effects of caffeic acid ester compounds **7** to **11**, which include various lengths of alkyl side chains, on HCV replication (Table 2 and Figure S2). The EC_{50} values decreased in the order methyl ester (compound **7**), n-butyl ester (compound **8**), n-hexyl ester (compound **9**), and n-octyl ester (compound **10**), suggesting that elongation of the n-alkyl side chain increased the inhibitory activity. However, the EC_{50} value of n-dodecyl ester (compound **11**) was higher than that of compound **10**. Thus, n-octyl ester (compound **10**) showed the lowest EC_{50} value and the highest SI among the tested compounds shown in Tables 1 and 2. Compounds **7** to **11** gradually increased own *Clog P* values,

Table 1. Effect of CAPE (**1**) and related compounds **2–6** on HCV replication.

Compound (Number)	EC_{50} [a] (μM)	CC_{50} [b] (μM)	SI [c]	*Clog P* [d]
CAPE (**1**)	9.0±0.7	136.1±1.9	17.9	3.30
caffeic acid (**2**)	36.6±6.7	>320	>8.7	0.98
ferulic acid (**3**)	71.9±5.8	>320	>4.5	1.42
cinnamic acid henethyl ester (**4**)	86.1±6.3	>320	>3.7	4.56
chlorogenic acid (**5**)	103.0±3.4	>320	>3.1	−0.96
rosmarinic acid (**6**)	109.6±1.1	>320	>2.9	1.10

a: Fifty percent effective concentration based on the inhibition of HCV replication.
b: Fifty percent cytotoxicity concentration based on the reduction in cell viability.
c: Selectivity index (CC_{50}/EC_{50}).
d: Determined with ChemDraw software (Chem Bio Office Ultra, 2008).
doi:10.1371/journal.pone.0082299.t001

corresponding to length of n-alkyl side chain (Fig. 2A). Compounds **10** and **11** exhibit EC_{50} values of 2.7 and 5.9 μM, respectively, SI values of 29.6 and 9.80, respectively, and *Clog P* values of 4.90 and 5.96, respectively, suggesting that high hydrophobic property of n-alkyl side chain decreases anti-HCV activity. The appropriate *Clog P* value of caffeic acid ester containing unsaturated side chain may be around 5.

Dihydrocaffeic acid methyl ester (compound **12**) showed less activity than caffeic acid methyl ester (compound **7**) regardless of values of *Clog P* value and CC_{50}, suggesting that the alpha, beta-unsaturated part attached to ester affects the anti-HCV activity level (Table 3 and Figure S3).

We further examined the effect of the hydroxyl groups on the aromatic ring on HCV replication (Table 4 and Figure S4). The EC_{50} values of *O*-methylated caffeic acid n-octyl esters (compounds **13** and **14**) were higher than that of compound **10**. Compounds **15** including 3, 4-di-*O*-methylated caffeic acid n-octyl ester exhibited higher EC_{50} than values of compounds **10**, **13** and **14**. However, addition of a third hydroxyl group to 3, 4, 5-trihydroxy derivative (compound **16**) of compound **10** resulted in a reduction of anti-HCV activity. Furthermore, *Clog P* values of compound **10**, **13**, **14, 15** and **16** were not correlated with anti-HCV activity (EC_{50} value) (Fig. 2B). These results suggest that the catechol moiety plays an important role in anti-HCV activity, and that the 4-hydroxy moiety is more important for the activity than the 3-hydroxy moiety.

Thus, compound **10**, which exhibits the lowest EC_{50} value and the highest SI value, is the most effective compound among CAPE analogues used in this study.

Effect of CAPE derivatives on virus production

The structure of compound **10** is shown in Fig. 3A. Treatment with compound **10** reduced HCV replication and NS3 protein in a dose-dependent manner at a higher anti-HCV level than

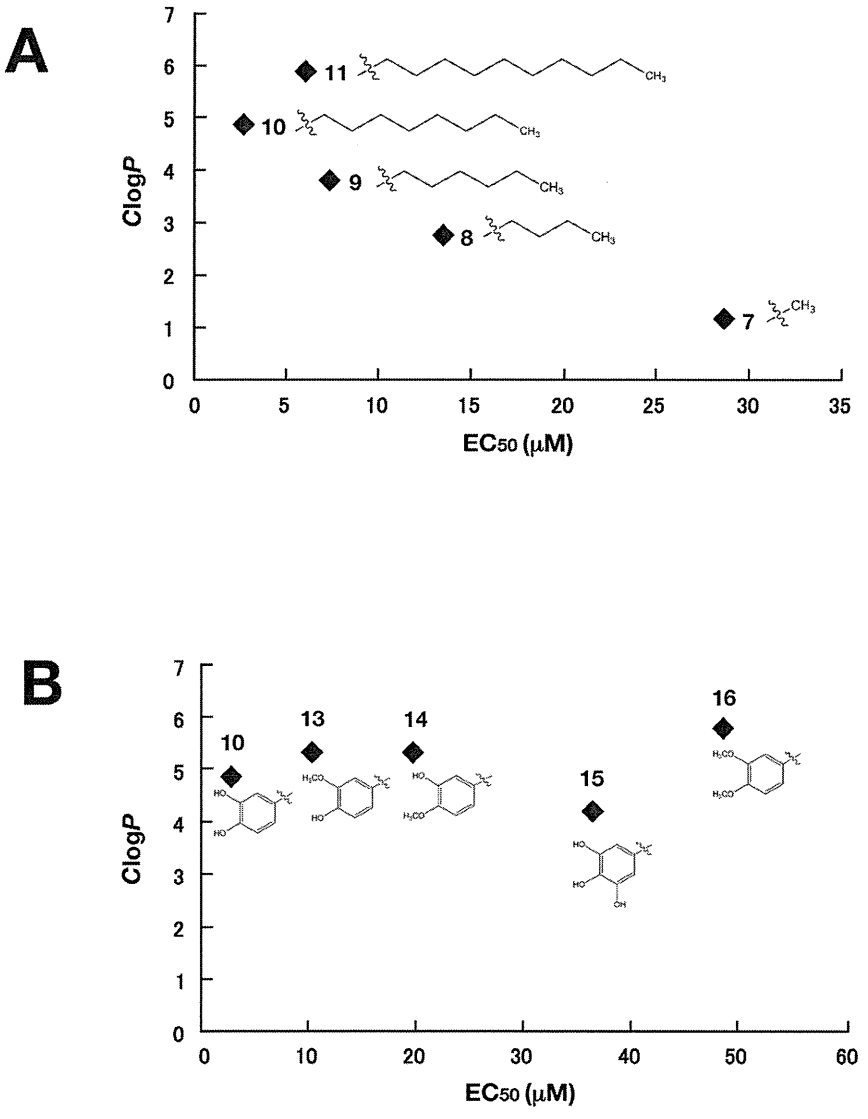

Figure 2. Correlation between the inhibitory effect on HCV replication *and* Clog *P* of CAPE analogues. Values of *x*-axis indicate EC_{50} values of CAPE analogues, while values of *y*-axis show *Clog P* values. (A) Correlation between the inhibitory effect on HCV replication and *Clog P* of CAPE analogues (Compound 7–11). (B) Correlation between the inhibitory effect on HCV replication and *Clog P* of CAPE analogues (Compound 10 and 13–16).
doi:10.1371/journal.pone.0082299.g002

Table 2. Effect of caffeic acid esters **7, 9–14**, including **1**, on HCV replication.

Compound No.	R	EC_{50} [a] (μM)	CC_{50} [b] (μM)	SI [c]	Clog *P* [d]
7	CH_3	28.6±1.2	122.1±5.0	4.2	1.20
8	C_4H_9	13.5±2.1	39.0±1.1	2.9	2.79
9	C_6H_{13}	7.3±0.2	37.6±1.2	5.1	3.85
10	C_8H_{17}	2.7±0.1	71.7±8.5	26.6	4.90
11	$C_{10}H_{21}$	5.9±0.9	57.9±2.9	9.8	5.96
1	$(CH_2)_2Ph$	9.0±0.7	136.1±1.9	17.9	3.30

The basic structure and side moieties are shown in Figure S2.
a: Fifty percent effective concentration based on the inhibition of HCV replication.
b: Fifty percent cytotoxicity concentration based on the reduction in cell viability.
c: Selectivity index (CC_{50}/EC_{50}).
d: Determined with ChemDraw software (Chem Bio Office Ultra, 2008).
doi:10.1371/journal.pone.0082299.t002

compound **1** (Figs. 3B and C), but not effect enzymatic activities of firefly and *Renilla* luciferases (Fig. 3D) and IRES-dependent translation (Fig. 3E), suggesting that inhibition of HCV replication by compound **10** is not due to offtarget effect. We evaluated the inhibitory effect of compound **10** on three different subgenomic replicon cell lines (1b: N strain, Con1 strain, 2a: JFH-1 strain) and one full genome replicon cell line (1b: O strain). Compound **10** inhibited the viral replication of all replicon cell lines at similar level, and exhibited the lowest EC_{50} value of 1.0 μM and an SI value of 63.1 by using Con1 replicon cells (Table 5). We next examined the effect of compound **10** on virus production by using HCVcc, since subgenomic replicon mimics HCV replication, but not the whole viral cycle. The Huh7 OK1 cell line, which is highly permissive to the HCV JFH1 strain [22], was infected with HCVcc and then treated with compound **10** at 24 h post-infection. The supernatant was harvested 72 h post-infection from the culture supernatant and then the RNA that prepared from the supernatant was estimated by real time qRT-PCR. Figure 3F shows that treatment with compound **10** reduced HCV viral production ($EC_{50} = 1.8 \pm 0.4$ μM) in a similar way to the data obtained by using a replicon cell line. To clarify whether or not compound **10** inhibited HCV replication via interferon-signaling pathway, we analyzed ISRE activity and the expression of interferon stimulated gene (ISG) by using reporter assay and RT-PCR, respectively. The replicon cells were harvested at 48 h post-treatment. There were no significant effects of compound **1**, **6** and **10** on ISRE-promoter activities, while interferon alpha 2b significantly enhanced it as a positive control (Fig.4 A). The data of the RT-PCR analysis showed that the transcriptional expressions of ISGs including Mx1, MxA, IFIT4, ISG15, OAS1, OAS2, and OAS3 were induced with interferon alpha 2b, but not with compound **1**, **6** and **10** (Fig. 4B). These data suggest that the CAPE derivatives have an inhibitory effect on virus production and replication, irrespective of interferon signaling induction.

Synergistic effect of caffeic acid n-octyl ester on interferon and direct-acting antiviral agents

To estimate the effects of drug combinations on anti-HCV activity, we examined the antiviral activity of compound **10** in combination with IFN-α 2b, telaprevir (NS3 protease inhibitor), danoprevir (NS3 protease inhibitor), daclatasvir (NS5A inhibitor) or VX-222 (NS5B polymerase inhibitor). Con1 LUN Sb #26 replicon cells were treated with compound **10** in combination with

Table 3. Effect of caffeic acid esters **7**and **8** on HCV replication.

Compound No.	EC_{50} [a] (μM)	CC_{50} [b] (μM)	SI [c]	Clog *P* [d]
7	28.6±1.2	122.1±5.0	4.2	1.20
12	77.0±1.6	140.7±3.4	1.8	1.02

Chemical structures of both compounds are shown in Figure S3
a: Fifty percent effective concentration based on the inhibition of HCV replication.
b: Fifty percent cytotoxicity concentration based on the reduction in cell viability.
c: Selectivity index (CC_{50}/EC_{50}).
d: Determined with ChemDraw software (Chem Bio Office Ultra, 2008).
doi:10.1371/journal.pone.0082299.t003

each anti-HCV agent at various concentration rations for 72 h. The effect of each drug combination on HCV replication was analyzed by using CalcuSyn. An explanatory diagram of isobologram was shown at a right end of lower panels of Fig. 5A as described in Materials and Methods. As shown in the resulting isobologram, all plots of the calculated EC_{90} values of compound **10** with IFN-alpha 2b, daclatasvir, or VX-222 are located under the additive line, while the plots of compound **10** with telaprevir, or danoprevir are located above the additive line and closed to the additive line (Fig. 5A). Additionally, we determined the degree of inhibition for each drug combination was analyzed as the combination index (CI) calculation at 50, 75 and 90% of effective concentrations by using CalcuSyn. An explanatory diagram was shown at a right end of lower panels of Fig. 5B as described in Materials and Methods. On the basis of the CalcuSyn analysis, the combination of compound **10** with daclatasvir exhibited strong synergistic effect on inhibition of HCV replication in the replicon cells (Fig. 5B, upper middle). The combination of compound **10** with VX-222 exhibited an additive to synergistic effect, suggesting that it trends toward synergistic (Fig. 5B, upper right), and with IFN-alpha 2b exhibited an antagonistic to synergistic effect, suggesting that it trends toward synergistic (Fig. 5B, upper left). In contrast, the combination of compound **10** with telaprevir resulted in antagonistic effect (Fig. 5B, lower left), and with danoprevir resulted in an antagonistic to additive effect, suggesting it trends toward antagonistic (Fig. 5B, lower middle). These calculated data

Table 4. Effect of octyl esters **10** and **13–16** on HCV replication.

Compound No.	R^1, R^2, R^3	EC_{50} [a] (μM)	CC_{50} [b] (μM)	SI [c]	Clog *P* [d]
10	$R^1=R^2=R^3=H$	2.7±0.1	71.7±8.5	26.6	4.90
13	$R^1=CH_3$, $R^2=R^3=H$	10.2±1.1	60.3±1.6	5.9	5.35
14	$R^1=R^3=H$, $R^2=CH_3$	19.6±0.8	59.2±1.4	3	5.35
15	$R^1=R^2=CH_3$, $R^3=H$	48.5±1.7	212.4±6.9	4.4	5.82
16	$R^1=R^2=H$, $R^3=OH$	36.3±2.9	59.8±6.9	1.6	4.24

The basic structure and side moieties are shown in Figure S4.
a: Fifty percent effective concentration based on the inhibition of HCV replication.
b: Fifty percent cytotoxicity concentration based on the reduction in cell viability.
c: Selectivity index (CC_{50}/EC_{50}).
d: Determined with ChemDraw software (Chem Bio Office Ultra, 2008).
doi:10.1371/journal.pone.0082299.t004

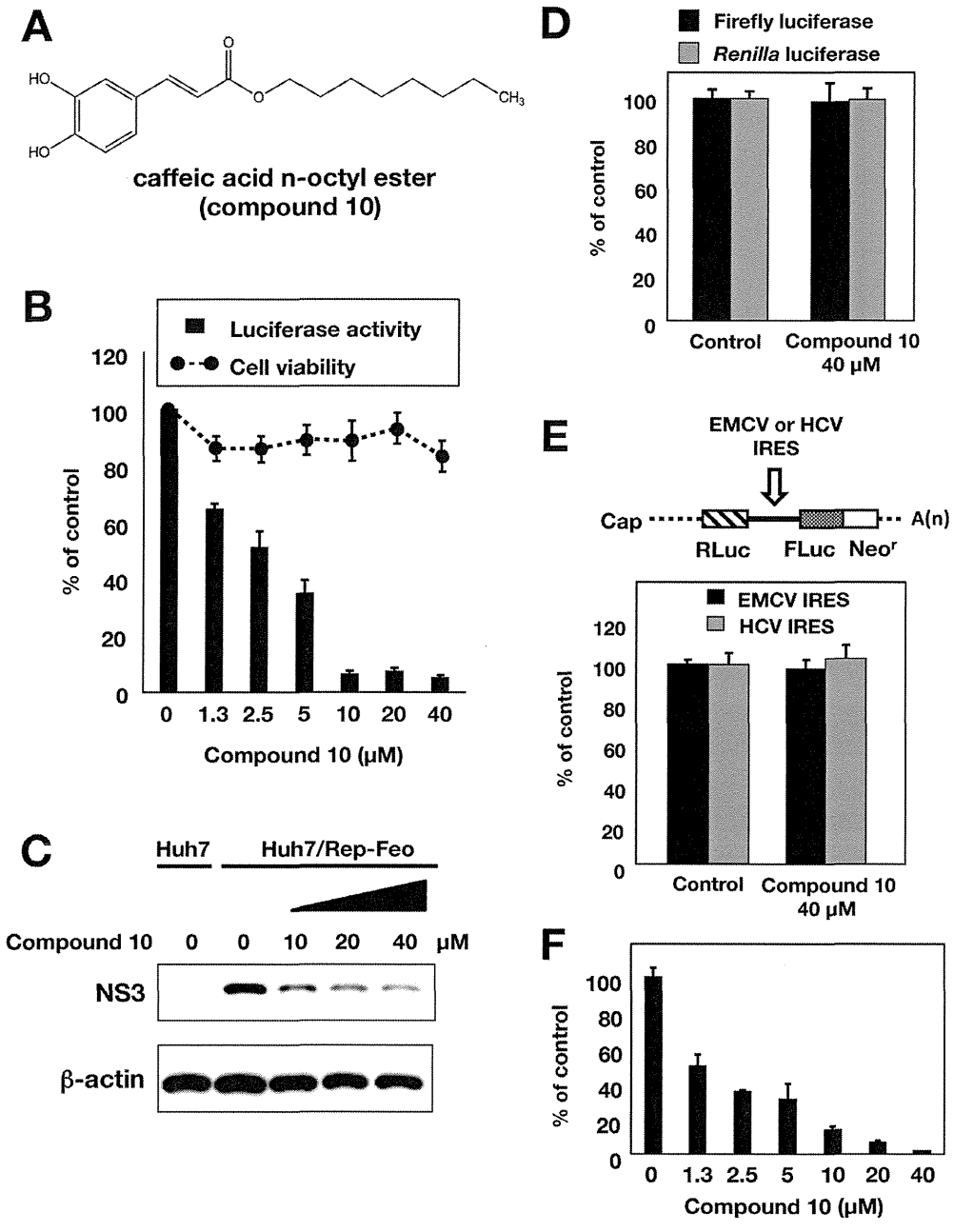

Figure 3. Effect of compound 10 on the viral replication in the replicon cell line and HCVcc. (A) Molecular structure of compound **10**. (B) Huh7/Rep-Feo cells were incubated for 72 h in a medium containing various concentrations of compound **10**. Luciferase and cytotoxicity assays were carried out by the method described in Materials and Methods. Error bars indicate standard deviation. The data represent three independent experiments. (C) Protein extract was prepared from Huh7/Rep-Feo cells treated for 72 h with the indicated concentration of compound **10** and it was then subjected to Western blotting using antibodies to NS3 and beta-actin. (D) Huh7 cell line was transfected with pEF Fluc IN encoding firefly luciferase or pEF Rluc IN encoding *Renilla* luciferase. Both transfected cell lines were incubated with DMSO (Control) or 40 μg/ml compound **10**. Firefly or *Renilla* luciferase activity was measured 72 h post-treatment. Luciferase activity was normalized with protein concentration. Error bars indicate standard deviation. The data were represented from three independent experiments. (E) Schematic structure of RNA transcribed from the plasmids was shown (Top). The bicistronic gene is transcribed under the control of elongation factor 1α (EF1α) promoter. The upstream cistron encoding *Renilla* luciferase (RLuc) is translated by a cap-dependent mechanism. The downstream cistron encodes the fusion protein (Feo), which consists of the firefly luciferase (Fluc) and neomycin phosphotransferase (Neo^r), and is translated under the control of the EMCV or HCV IRES. Huh7 cell line was transfected with each plasmid and incubated for 72 h post-treatment with DMSO (control) or 40 μg/ml of compound **10**. Firefly and *Renilla* luciferase activities were measured. Relative ratio of Firefly luciferase activity to *Renilla* luciferase activity was represented as percentage of the control condition. Error bars indicate standard deviation. The data were represented from three independent experiments. (F) Huh7 OK1 cell line was infected with HCVcc derived from JFH-1 strain and then treated with several concentrations of compound **10** at 24 h post-infection. The resulting cells were harvested 72 h post-infection. The viral RNA of supernatant was purified and estimated by the method described in Materials and Methods. Error bars indicate standard deviation. The data represent three independent experiments. Treatment with DMSO corresponds to '0'.
doi:10.1371/journal.pone.0082299.g003

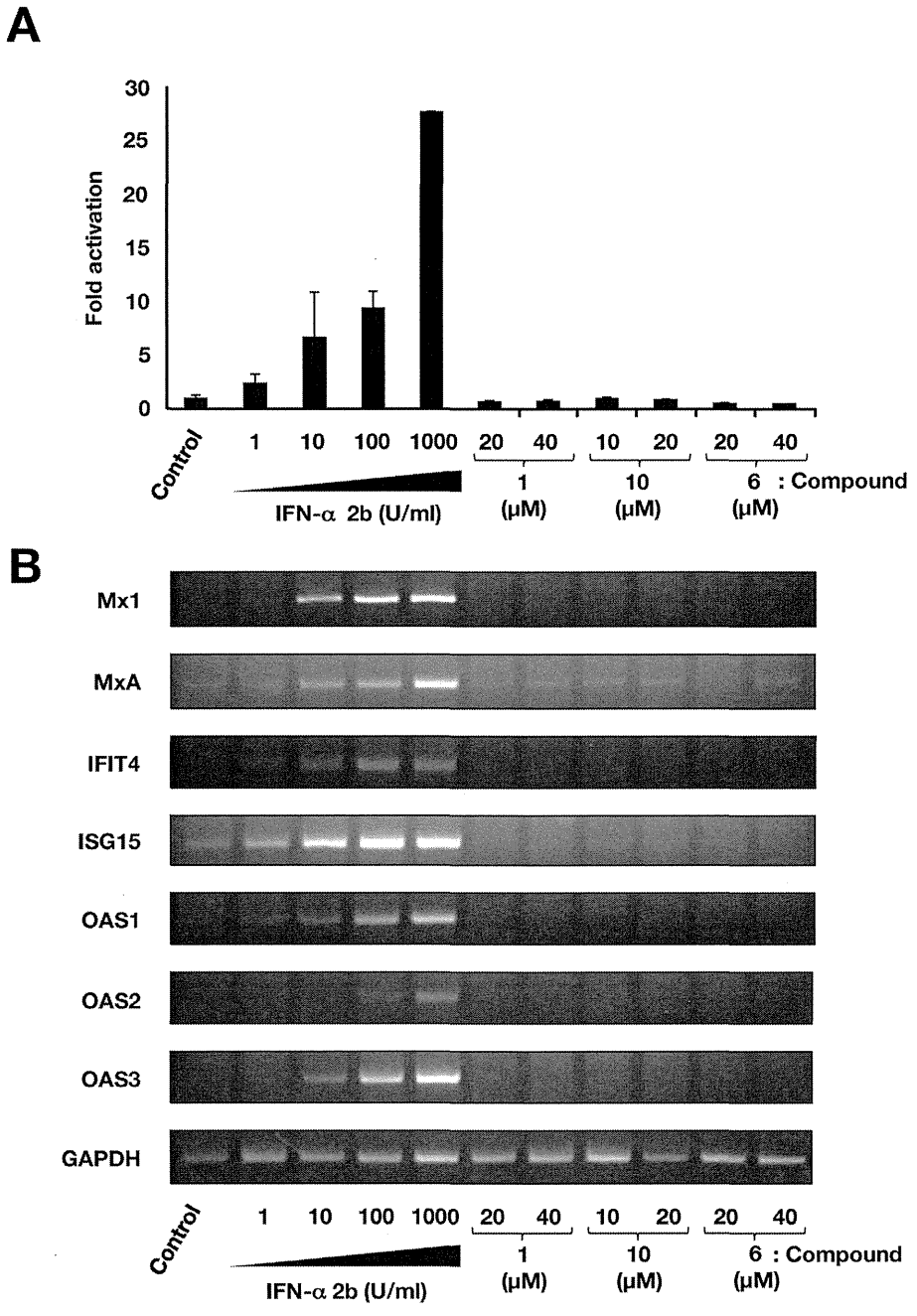

Figure 4. Effect of CAPE derivatives on the interferon-signaling pathway. (A) Plasmids pISRE-TA-Luc and phRG-TK were co-transfect into Huh7 OK1 cells. The transfected cells were cultured with 1, 10, 100, or 1000 U/mL of interferon-alpha 2b, and compounds **1**, **6** and **10**. Treatment with DMSO corresponds to '0'. After 48 h of treatment, luciferase activities were measured, and the value were normalized against *Renilla* luciferase activities. Error bars indicate standard deviation. The data represent three independent experiments. (B) Huh7 replicon cell line of genotype 1b was treated with 1, 10, 100, or 1000 U/mL of interferon-alpha 2b, and compounds **1**, **6** and **10** for 48 h. Treatment with DMSO corresponds to the control. The mRNAs of Mx1, MxA, IFIT4, ISG15, OAS1, OAS2, OAS3, and GAPDH as an internal control were detected by RT-PCR.
doi:10.1371/journal.pone.0082299.g004

of combination tests suggest that daclatasvir, IFN-alpha 2b, and VX-222 synergistically, but telaprevir and danoprevir antagonistically, inhibit HCV replication in combination with compound **10**.

Discussion

CAPE is an active component of propolis, which possesses broad-spectrum biological activities [14–19]. In this study, CAPE suppressed HCV RNA replication in a dose-dependent manner (Fig. 1A and B). Treatment with CAPE inhibited HCV replication with an EC_{50} of 9.0 μM and an SI of 17.9 in Huh7/Rep-Feo cells (Table 1). The treatment of the replicon cell line with CAPE did not induce expression of the IFN-inducible gene (Fig. 4), suggesting that the inhibition of HCV replication by CAPE is independent of the IFN signaling pathway.

Table 5. Anti-HCV activity of compound **10** in replicon cell lines of genotypes 1b and 2a.

Cell line	Replicon type	Strain (Genotype)	EC_{50} [a] (μM)	CC_{50} [b] (μM)	SI [c]
Huh7 Rep/Feo-1b	Subgenome	N (1b)	2.7±0.1	71.7±8.5	26.6
Con1 LUN Sb #26	Subgenome	Con1 (1b)	1.0±0.1	63.1±3.1	63.1
Huh7 Rep/Reo-2a	Subgenome	JFH1 (2a)	1.0±0.3	60.0±2.3	60.0
OR6	Full genome	O (1b)	1.5±0.4	61.7±0.6	41.1

a: Fifty percent effective concentration based on the inhibition of HCV replication.
b: Fifty percent cytotoxicity concentration based on the inhibition of HCV replication.
c: Selectivity Index (CC_{50}/EC_{50}).
doi:10.1371/journal.pone.0082299.t005

We also examined the effect of CAPE derivatives on HCV replication. Our data suggest that the n-alkyl side chain and catechol moiety of the CAPE derivative are critical in its anti-HCV activity (Tables 2 and 3). The EC_{50} value of the derivative decreased dependently on the length of the n-alkyl side chain until reaching octyl ester length (Table 2), while longer chains than octyl ester of a derivative led to an increase in the EC_{50} value and *Clog P* value. Compound **10**, Caffeic acid n-octyl ester, exhibited the highest anti-HCV activity among the tested compounds with an EC_{50} value of 2.7 μM and an SI value of 26.6. Cyclosporine A and its analogues could suppress the viral replication of genotype 1b at a higher level than that of genotype 2a [23]. Interestingly, compound **10** could inhibit HCV replication of genotype 1b and 2a at a similar level, irrespective of expression of the interferon-inducible gene (Fig. 4). CAPE and its derivatives may therefore possess a mechanism different from cyclosporine A and its analogues with respect to anti-HCV activity.

CAPE has been reported to be an inhibitor of NF-kappaB [14,20]. Lee et al. reported that the catechol moiety in CAPE was important for inhibition of NF-kappaB activation [24]. The data shown in Table 3 suggest that the catechol moiety in CAPE is critical to the anti-HCV activity of compound **10**. Previous studies have implicated the inhibition of NF-kappaB in anti-HCV activity. Treatment with an extract prepared from *Acacia confusa* [25] or San-Huang-Xie-Xin-Tang [26] could suppress HCV replication and inhibit NF-kappaB activation. However, Chen et al. reported that curcumin-mediated inhibition of NF-kappaB did not contribute to anti-HCV activity [11]. Furthermore, treatment with *N*′-(Morpholine-4carbonyloxy)-2(naphthalene-1-yl) acetimidamide could activate NF-kappaB and downstream gene expression in the same Huh7/Rep-Feo replicon cell line as the cell line used in this study and exhibited potent inhibition of HCV replication without interferon signaling [27]. These reports support the notion that CAPE derivatives do not mainly target NF-kappaB activity as part of their anti-HCV activity.

Several host proteins have been reported to regulate function of NS5A, leading to supporting HCV replication (review in [2,28]). Daclatasvir exhibited potent synergistic effect on anti-HCV activity in combination of compound **10** (Fig. 5). Anti-HCV activity of compound **10** might associate with intrinsic functions of host factors that interact with NS5A. NS3 protease inhibitors exhibited antagonistic effect in combination of compound **10** (Fig. 5). The inhibitory effect of compound **10** might be mediated by the activation of an unknown endogenous protease that is nonspecifically suppressed by NS3 protease inhibitors. Further study to clarify the mechanism by which compound **10** suppresses HCV replication might contribute to identification of a novel host factor as a drug target for development of the effective compound supporting an effect of other anti-HCV drugs.

In conclusion, we showed that CAPE and its analogue possess a significant inhibitory effect against HCV replication. The length of n-alkyl side chains and the catechol moiety of CAPE are critical to its inhibitory activity against HCV replication. The most effective derivative among the tested compounds was caffeic acid n-octyl ester, which exhibited an EC_{50} value of 1 μM and an SI value of 63.1 in the replicon cell line of genotype 1b strain Con1. Treatment with caffeic acid n-octyl ester reduced the viral replication of genotype 1b and 2a at a similar level and inhibited viral production of HCVcc. Treatment with caffeic acid n-octyl ester could synergistically enhance the anti-HCV activities of IFN-α 2b, daclatasvir, and VX-222, but neither telaprevir nor danoprevir. Further investigation to clarify the mechanism of anti-HCV activity and further modification of the compound to improve anti-HCV activity will lead to novel therapeutic strategies to treat chronic hepatitis C virus infection.

Materials and Methods

Compounds

Boldface numbers in this text indicate the compound numbers shown in Tables. All chemical structures of compounds used in this study are shown in figure S1. CAPE (**1**), caffeic acid (**2**), ferulic acid (**3**), and chlorogenic acid (**5**) and were purchased from Sigma-Aldrich (St. Louis, MO, USA). Cinnamic acid phenethyl ester (**4**) was from Tokyo Chemical Industry (Tokyo, Japan). Rosmarinic acid (**6**) was from Wako Pure Chemical (Tokyo, Japan). Caffeic acid n-octyl ester (n-octyl caffeate) (**10**), 3-O-methylcaffeic acid n-octyl ester (n-octyl-3-methylcaffeate) (**13**), 4-O-methylcaffeic acid n-octyl ester (n-octyl-3-methylcaffeate) (**14**), and 3, 4-O-dimethyl-caffeic acid n-octyl ester (n-octyl-3, 4-methylcaffeate) (**15**) were from LKT Laboratories (St. Paul, MN, USA).

Caffeic acid esters **7**, **8**, **9**, and **11** were synthesized by preparing caffeic acid chloride followed by treatment with corresponding alcohols [29]. Dihydrocaffeic acid ester **12** was prepared by hydrogenation of **7**. Compound **16** is a newly synthesized ester. Spectroscopic data of known esters **7–9**, and **11** prepared here were identical to those reported [30-32] Interferon alfa-2b (IFN-α 2b) was obtained from MSD (Tokyo, Japan). Telaprevir and daclatasvir were purchased from Selleckchem (Houston, TX, USA). Danoprevir and VX-222 were from AdooQ BioScience (Irvine, CA, USA).

Chemistry of 3,4,5-Trihydroxycinnamic acid n-octyl ester

3,4,5-Trihydroxycinnamic acid n-octyl ester (**16**) was prepared by condensation of corresponding benzaldehydes with malonic acid n-octyl monoester [33]. A solution of malonic acid n-octyl monoester (432 mg, 2 mmol), 3,4,5-trihydroxybenzaldehyde (462 mg, 3 mmol) and piperidine (0.2 mL) in pyridine (2 mL)

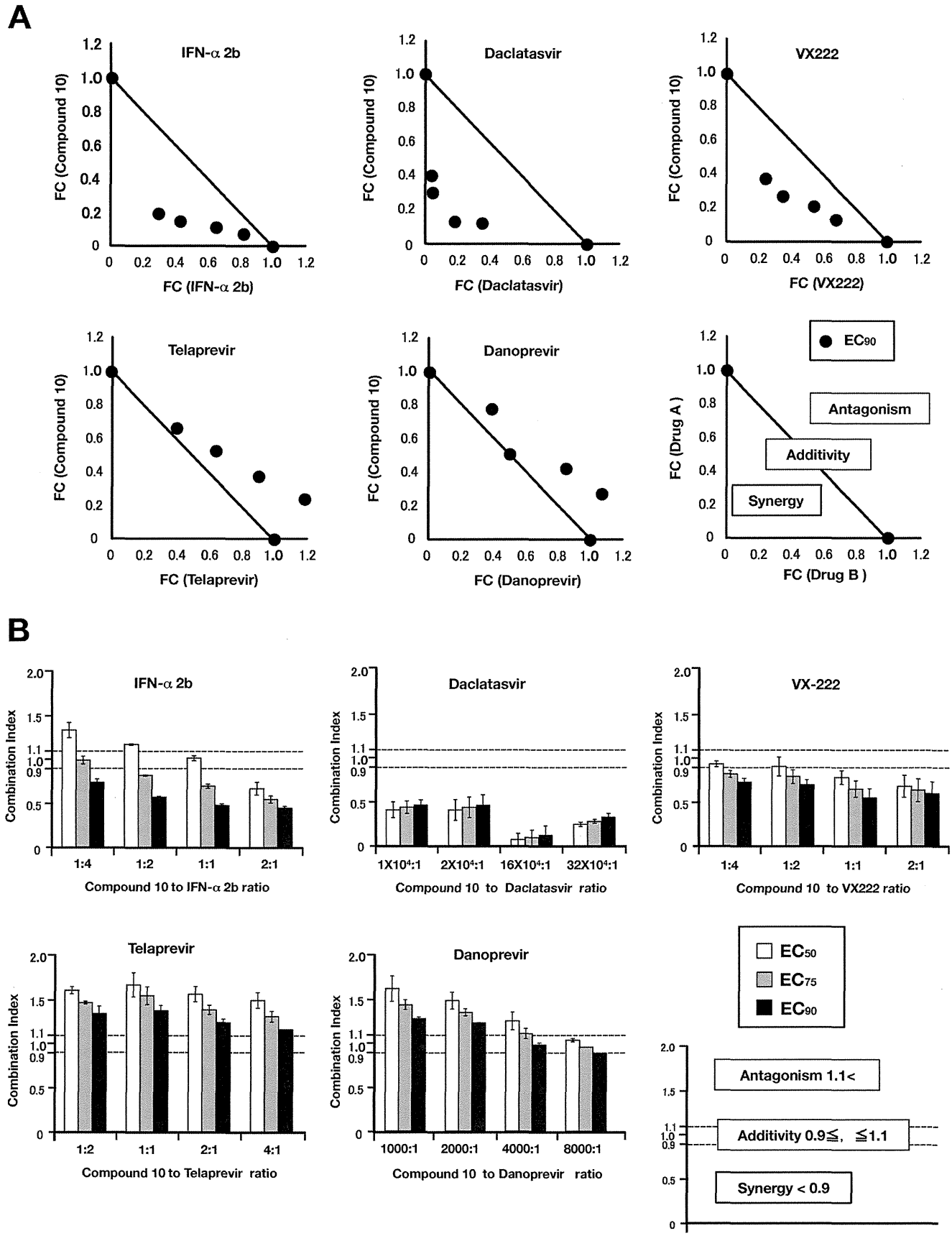
A
IFN-α 2b
FC (Compound 10)
FC (IFN-α 2b)
Daclatasvir
FC (Daclatasvir)
VX222
FC (VX222)
Telaprevir
FC (Telaprevir)
Danoprevir
FC (Danoprevir)
EC90
Antagonism
Additivity
Synergy
FC (Drug A)
FC (Drug B)
B
IFN-α 2b
Combination Index
Compound 10 to IFN-α 2b ratio
Daclatasvir
Compound 10 to Daclatasvir ratio
VX-222
Compound 10 to VX222 ratio
Telaprevir
Compound 10 to Telaprevir ratio
Danoprevir
Compound 10 to Danoprevir ratio
EC50
EC75
EC90
Antagonism 1.1<
Additivity 0.9≦, ≦1.1
Synergy < 0.9

Figure 5. Synergistic effect analyses for the combination of compound 10 with IFN-α 2b, daclatasvir, VX-222, telaprevir, or danoprevir. The Huh7 cell line, including the subgenomic replicon RNA of genotype 1b strain Con1, was treated for 72h with combinations of compound 10 and IFN-α 2b, daclatasvir, VX-222, telaprevir, or danoprevir. Luciferase assay were carried out as described in Materials and Methods. (A) The calculated EC_{90} values for combination were plotted as the fractional concentration (FC) of compound 10 and one of IFN-α 2b, daclatasvir, VX-222, telaprevir, and danoprevir on the *x* and *y* axes, respectively. Synergy, antagonism and additivity are indicated in a representative graph as a right end of lower graphs and are described in Materials and Methods. (B) Combination indexes of compound 10 with IFN-α 2b, daclatasvir, VX-222, telaprevir, or danoprevir at the EC50, EC75, and EC90 values were measured at various drug rations. Synergy, antagonism and additivity are indicated in a representative graph as a right end of lower graphs and are described in Materials and Methods.
doi:10.1371/journal.pone.0082299.g005

was heated at 70°C for 1 h. The reaction mixture was concentrated under a vacuum to give a residue, which was dissolved in $CHCl_3$-IPA (3:1, v/v) and then washed with 10% HCl and water. The organic layer was dried over Na_2SO_4 and evaporated to give a residue, which was purified by silica gel column chromatography using AcOEt-hexane (1:1, v/v) as eluent to give the corresponding n-octyl ester (85 mg, 13.8%) as a pale powder. FT-IR vmax (KBr): 3389, 3239, 2923, 1675, 1627, 1606 cm^{-1}. ^1H NMR (400MHz, CD_3OD) δ: 0.86 (3H, t, J= 7.2 Hz), 1.20–1.40 (10H, m), 1.65 (2H, quintet, J= 6.4 Hz), 4.11, (2H, t, J= 6.4 Hz), 6.16 (2H, d, J= 15.6 Hz), 6.55 (2H, s), 7.40 (2H, d, J= 15.6 Hz). 13C NMR (100 Hz, CD_3OD) δ: 14.4, 23.7, 27.1, 29.8, 30.3, 30.4, 32.9, 65.6, 108.5, 115.3, 126.6, 137.5, 147.1, 169.4. CI MS *m/z*: 309 (M^++H). High-resolution CI MS calcd. for $C_{17}H_{25}O_5$ (M^++H) for 309.1702. Found: 309.1686.

Replicon cell lines and virus infection

The Huh7/Rep-Feo cell line, which harbors the subgenomic replicon RNA composed of HCV IRES, the gene of the fusion protein consisting of neomycin phosphotransferase and firefly luciferase, EMCV IRES and a nonstructural gene of genotype 1b strain N in order in Huh7 cell line, was previously established [34]. Thus, the luciferase activity corresponds to the level of HCV RNA replication. The cell line was maintained in Dulbecco's modified Eagle medium containing 10% fetal calf serum and 0.5 mg/mL G418 and cultured in absence of G418 when they were treated with compounds. The Lunet/Con1LUN Sb #26 cell line, which harbors the subgenomic replicon RNA of the Con1 strain (genotype 1b), was described previously [35]. The OR6 cell line, which harbors the full genomic replicon RNA of the O strain (genotype 1b), was described previously [36]. The HCV replicon cell line derived from the genotype 2a strain JFH1 was described previously [37]. The viral RNA derived from the plasmid pJFH1 was transcribed and introduced into Huh7OK1 cells according to the method of Wakita et al. [38]. The virus was amplified by the several times passages. The cells were infected with the virus at a multiplicity of infection (moi) of 1 and then treated with each compound at 24 h post-infection. The culture supernatants were harvested 72 h post-treatment to estimate the viral RNA as described below.

Determination of luciferase activity in HCV replicon cells

The replicon cells were seeded at 2×10^4 cells per well in a 48-well plate 24 h before treatment. Compounds were added to the culture medium to give various concentrations. The resulting cells were harvested 72 h post-treatment and lysed with cell culture lysis reagent (Promega, Madison, WI). The luciferase activity of each cell lysate was estimated using a luciferase assay system (Promega). The resulting luminescence was detected by a Luminescencer-JNR AB-2100 (ATTO, Tokyo, Japan).

Determination of Cytotoxicity in HCV replicon cells

The replicon cells were seeded at a density of 1×10^4 cells per well in a 96-well plate and then incubated at 37°C for 24 h. Compounds were added to the culture medium to give various concentrations and were then harvested 72 h post-treatment. Cell viability was measured using a dimethylthiazol carboxymethoxyphenylsulfophenyl tetrazolium (MTS) assay with a CellTiter 96 aqueous one-solution cell proliferation assay kit (Promega).

Western Blotting

Western blotting was carried out by the method described previously [39]. The antibodies to NS3 (clone 8G-2, mousemonoclonal, Abcam, Cambridge, UK), and beta-actin were purchased from Cell Signaling Technology (rabbit polyclonal, Danvers, MA, USA) and were used as the primary antibodies in this study.

RNA analysis

Total RNAs were prepared from cells by using the RNAqueous-4PCR kit (Life Technologies, Carlsbad, CA). Viral RNA were prepared from culture supernatants by using the QIAamp Viral RNA mini kit (QIAGEN, Hilden, Germany). The viral RNA genome was estimated by the qRT-PCR method described previously [40]. RT-PCR was carried out by the method described previously [41] which was slightly modified at the PCR step. The PCR samples were incubated once for 10 min at 95°C for an initial activation step of the AmpliTaq Gold DNA Polymerase (Life Technologies), and then subjected to an amplification step of 30 repeats of the cycle consisting of three segments as follow: 0.5 min at 95°C, 1 min at 55°C and 1 min at 72°C. The primers used in this study were as follows: Mx1: 5′-AGCCACTGGACTGACGACTT-3′ and 5′-GAGGGCTGAAAATCCCTTTC-3′;

MxA: 5′-GTCAGGAGTTGCCCTTCCCA-3′ and 5′-ATTCCCATTCCTTCCCCGG-3′;

IFIT4: 5′-CCCTTCAGGCATAGGCAGTA-3′ and 5′-CTCCTACCCGTCACAACCAC -3′; ISG15: 5′-CGCAGATCACCCAGAAGAT-3′ and 5′-GCCCTTGTTATTCCTCACCA-3′;

OAS1: 5′-CAAGCTCAAGAGCCTCATCC-3′ and 5′-TGGGCTGTGTTGAAATGTGT-3′;

OAS2: 5′-ACAGCTGAAAGCCTTTTGGA-3′ and 5′-GCATTAAAGGCAGGAAGCAC-3′;

OAS3: 5′-CACTGACATCCCAGACGATG-3′ and 5′-GATCAGGCTCTTCAGCTTGGC-3′;

GAPDH: 5′-GAAGGTGAAGGTCGGAGTC and 5′- GAAGATGGTGATGGGATTTC-3′

Effects on activities of internal ribosome entry site (IRES) and luciferases

Huh7 OK1 cells were transfected with pEF.Rluc.HCV.IRES.-Feo or pEF.Rluc.EMCV.IRES.Feo [39]. These transfected cells were seeded at 2×10^4 cells per well in a 48-well plate 24 h before treatment, treated with DMSO or compound **10**, and then harvested at 72 h post-treatment. The firefly luciferase activities were measured with a luciferase assay system (Promega). The total protein concentration was measured using the BCA Protein Assay Reagent Kit (Thermo Scientific, Rockford, IL, USA) to normalize

luciferase activity. To evaluate the interferon response, Huh7OK1 cells were seeded on a 48 well plate at a density of 2×10^4 cells per well, and transfected with pISRE-TA-Luc (Takara bio, Shiga, Japan) and phRG-TK (Promega). These transfected cells were incubated in the presence of compounds, IFN-α 2b, or DMSO, and then harvested at 48 h post-treatment. The firefly luciferase and *Renilla* luciferase activities were quantified by using Dual luciferase reporter assay system (Promega).

Prediction of Clog*P* for compounds

The *Clog*P value deduced from chemical structure roughly corresponds to a value of hydrophobicity. The *Clog*P values of compounds used in this study were calculated using the computer software Chem Bio Office Ultra 2008 (PerkinElmer, Cambridge, MA, USA).

Synergistic effect of caffeic acid n-octyl ester on anti-HCV activities of other drugs

The effects of drug-drug combinations were evaluated by using the Con1 LUN Sb #26 replicon cells, and were analyzed by using the computer software CalcuSyn (Biosoft, Cambridge, United Kingdom). Dose inhibition curves of two different drugs were plotted with each other. In each drug combination, EC_{90} values of several combinations of two different drugs were plotted as the fractional concentration (FC) of both drugs on the *x* and *y*-axes. Additivity indicates the line linked between 1.0 FC value points of both drugs in the absence of each other. Synergy and antagonism are indicated by values plotted under and above, respectively, an additivity line. The explanatory diagram of isobologram is shown in a right end of lower panels of Figure 5A. Combination indexes (CIs) were calculated at the EC_{50}, EC_{75}, and EC_{90} by using CalcuSyn. A CI value of less than 0.9 indicates synergy. A CI value ranging from 0.9 to 1.1 indicates additivity. A CI value of more than 1.1 indicates antagonism. The explanatory diagram was shown in a right end of lower panels of Figure 5B.

Supporting Information

Figure S1 Molecular structure of CAPE and commercial CAPE-related compounds. CAPE structure is divided into three parts: (I) the catechol moiety, (II) the alkenyl moiety on alpha, beta -unsaturated ester, and (III) the ester part. Molecular structures of CAPE and its commercial derivatives are shown.
(TIF)

Figure S2 The basic structure and side moieties of compounds shown in Table 2. Each compound structure is represented on the basis of the basic structure (top).
(TIF)

Figure S3 The molecular structures of compounds 7 and 12, which are shown in Table 3. Both compounds are different in alpha, beta-unsaturated or saturated part attached to ester.
(TIF)

Figure S4 The basic structure and side moieties of compounds shown in Table 4. Each compound structure is represented on the basis of the basic structure (top).
(TIF)

Acknowledgments

We thank T. Wakita for kindly providing a plasmid.

Author Contributions

Conceived and designed the experiments: MT KM. Performed the experiments: H. Shen AY MN HY MS H. Shindo SM. Analyzed the data: HK TT NE. Contributed reagents/materials/analysis tools: YF MI NK NS. Wrote the paper: H. Shen AY MT KM.

References

1. Baldo V, Baldovin T, Trivello R, Floreani A (2008) Epidemiology of HCV infection. Curr Pharm Des 14: 1646–1654.
2. Moriishi K, Matsuura Y (2012) Exploitation of lipid components by viral and host proteins for hepatitis C virus infection. Front Microbiol 3: 54.
3. Hijikata M, Kato N, Ootsuyama Y, Nakagawa M, Shimotohno K (1991) Gene mapping of the putative structural region of the hepatitis C virus genome by in vitro processing analysis. Proc Natl Acad Sci USA 88: 5547–5551.
4. Lohmann V, Korner F, Koch J, Herian U, Theilmann L, et al. (1999) Replication of subgenomic hepatitis C virus RNAs in a hepatoma cell line. Science 285: 110–113.
5. Hofmann WP, Zeuzem S (2011) A new standard of care for the treatment of chronic HCV infection. Nat Rev Gastroenterol Hepatol 8: 257–264.
6. Jacobson IM, McHutchison JG, Dusheiko G, Di Bisceglie AM, Reddy KR, et al. (2011) Telaprevir for previously untreated chronic hepatitis C virus infection. N Engl J Med 364: 2405–2416.
7. Sarrazin C, Hezode C, Zeuzem S, Pawlotsky JM (2012) Antiviral strategies in hepatitis C virus infection. J Hepatol 56 Suppl 1: S88–100.
8. Kieffer TL, Kwong AD, Picchio GR (2010) Viral resistance to specifically targeted antiviral therapies for hepatitis C (STAT-Cs). J Antimicrob Chemother 65: 202–212.
9. Ahmed-Belkacem A, Ahnou N, Barbotte L, Wychowski C, Pallier C, et al. (2010) Silibinin and related compounds are direct inhibitors of hepatitis C virus RNA-dependent RNA polymerase. Gastroenterology 138: 1112–1122.
10. Calland N, Albecka A, Belouzard S, Wychowski C, Duverlie G, et al. (2012) (-)-Epigallocatechin-3-gallate is a new inhibitor of hepatitis C virus entry. Hepatology 55: 720–729.
11. Chen MH, Lee MY, Chuang JJ, Li YZ, Ning ST, et al. (2012) Curcumin inhibits HCV replication by induction of heme oxygenase-1 and suppression of AKT. Int J Mol Med 30: 1021–1028.
12. Bachmetov L, Gal-Tanamy M, Shapira A, Vorobeychik M, Giterman-Galam T, et al. (2012) Suppression of hepatitis C virus by the flavonoid quercetin is mediated by inhibition of NS3 protease activity. J Viral Hepat 19: e81–88.
13. Takeshita M, Ishida Y, Akamatsu E, Ohmori Y, Sudoh M, et al. (2009) Proanthocyanidin from blueberry leaves suppresses expression of subgenomic hepatitis C virus RNA. J Biol Chem 284: 21165–21176.
14. Toyoda T, Tsukamoto T, Takasu S, Shi L, Hirano N, et al. (2009) Anti-inflammatory effects of caffeic acid phenethyl ester (CAPE), a nuclear factor-kappaB inhibitor, on Helicobacter pylori-induced gastritis in Mongolian gerbils. Int J Cancer 125: 1786–1795.
15. Ho CC, Lin SS, Chou MY, Chen FL, Hu CC, et al. (2005) Effects of CAPE-like compounds on HIV replication in vitro and modulation of cytokines in vivo. J Antimicrob Chemother 56: 372–379.
16. Chiao C, Carothers AM, Grunberger D, Solomon G, Preston GA, et al. (1995) Apoptosis and altered redox state induced by caffeic acid phenethyl ester (CAPE) in transformed rat fibroblast cells. Cancer Res 55: 3576–3583.
17. Boudreau LH, Maillet J, LeBlanc LM, Jean-Francois J, Touaibia M, et al. (2012) Caffeic acid phenethyl ester and its amide analogue are potent inhibitors of leukotriene biosynthesis in human polymorphonuclear leukocytes. PLoS One 7: e31833.
18. Lee KW, Chun KS, Lee JS, Kang KS, Surh YJ, et al. (2004) Inhibition of cyclooxygenase-2 expression and restoration of gap junction intercellular communication in H-ras-transformed rat liver epithelial cells by caffeic acid phenethyl ester. Ann N Y Acad Sci 1030: 501–507.
19. Fesen MR, Kohn KW, Leteurtre F, Pommier Y (1993) Inhibitors of human immunodeficiency virus integrase. Proc Natl Acad Sci U S A 90: 2399–2403.
20. Natarajan K, Singh S, Burke TR Jr, Grunberger D, Aggarwal BB (1996) Caffeic acid phenethyl ester is a potent and specific inhibitor of activation of nuclear transcription factor NF-kappa B. Proc Natl Acad Sci U S A 93: 9090–9095.
21. Li Y, Zhang T, Douglas SD, Lai JP, Xiao WD, et al. (2003) Morphine enhances hepatitis C virus (HCV) replicon expression. Am J Pathol 163: 1167–1175.
22. Okamoto T, Omori H, Kaname Y, Abe T, Nishimura Y, et al. (2008) A single-amino-acid mutation in hepatitis C virus NS5A disrupting FKBP8 interaction impairs viral replication. J Virol 82: 3480–3489.
23. Ishii N, Watashi K, Hishiki T, Goto K, Inoue D, et al. (2006) Diverse effects of cyclosporine on hepatitis C virus strain replication. J Virol 80: 4510–4520.

24. Lee Y, Shin DH, Kim JH, Hong S, Choi D, et al. (2010) Caffeic acid phenethyl ester-mediated Nrf2 activation and IkappaB kinase inhibition are involved in NFkappaB inhibitory effect: structural analysis for NFkappaB inhibition. Eur J Pharmacol 643: 21–28.
25. Lee JC, Chen WC, Wu SF, Tseng CK, Chiou CY, et al. (2011) Anti-hepatitis C virus activity of Acacia confusa extract via suppressing cyclooxygenase-2. Antiviral Res 89: 35–42.
26. Lee JC, Tseng CK, Wu SF, Chang FR, Chiu CC, et al. (2011) San-Huang-Xie-Xin-Tang extract suppresses hepatitis C virus replication and virus-induced cyclooxygenase-2 expression. J Viral Hepat 18: e315–324.
27. Kusano-Kitazume A, Sakamoto N, Okuno Y, Sekine-Osajima Y, Nakagawa M, et al. (2012) Identification of novel N-(morpholine-4-carbonyloxy) amidine compounds as potent inhibitors against hepatitis C virus replication. Antimicrob Agents Chemother 56: 1315–1323.
28. Moradpour D, Penin F, Rice CM (2007) Replication of hepatitis C virus. Nat Rev Microbiol 5: 453–463.
29. Lee YJ, Liao PH, Chen WK, Yang CY (2000) Preferential cytotoxicity of caffeic acid phenethyl ester analogues on oral cancer cells. Cancer Lett 153: 51–56.
30. Bourne GT, Golding SW, McGeary RP, Meutermans WD, Jones A, et al. (2001) The development and application of a novel safety-catch linker for BOC-based assembly of libraries of cyclic peptides. J Org Chem 66: 7706–7713.
31. Nagaoka T, Banskota AH, Tezuka Y, Saiki I, Kadota S (2002) Selective antiproliferative activity of caffeic acid phenethyl ester analogues on highly liver-metastatic murine colon 26-L5 carcinoma cell line. Bioorg Med Chem 10: 3351–3359.
32. Uwai K, Osanai Y, Imaizumi T, Kanno S, Takeshita M, et al. (2008) Inhibitory effect of the alkyl side chain of caffeic acid analogues on lipopolysaccharide-induced nitric oxide production in RAW264.7 macrophages. Bioorg Med Chem 16: 7795–7803.
33. Zhang Z, Xiao B, Chen Q, Lian XY (2010) Synthesis and biological evaluation of caffeic acid 3,4-dihydroxyphenethyl ester. J Nat Prod 73: 252–254.
34. Yokota T, Sakamoto N, Enomoto N, Tanabe Y, Miyagishi M, et al. (2003) Inhibition of intracellular hepatitis C virus replication by synthetic and vector-derived small interfering RNAs. EMBO Rep 4: 602–608.
35. Frese M, Barth K, Kaul A, Lohmann V, Schwarzle V, et al. (2003) Hepatitis C virus RNA replication is resistant to tumour necrosis factor-alpha. Journal of General Virology 84: 1253–1259.
36. Ikeda M, Abe K, Dansako H, Nakamura T, Naka K, et al. (2005) Efficient replication of a full-length hepatitis C virus genome, strain O, in cell culture, and development of a luciferase reporter system. Biochem Biophys Res Commun 329: 1350–1359.
37. Nishimura-Sakurai Y, Sakamoto N, Mogushi K, Nagaie S, Nakagawa M, et al. (2010) Comparison of HCV-associated gene expression and cell signaling pathways in cells with or without HCV replicon and in replicon-cured cells. J Gastroenterol 45: 523–536.
38. Wakita T, Pietschmann T, Kato T, Date T, Miyamoto M, et al. (2005) Production of infectious hepatitis C virus in tissue culture from a cloned viral genome. Nat Med 11: 791–796.
39. Yamashita A, Salam KA, Furuta A, Matsuda Y, Fujita O, et al. (2012) Inhibition of hepatitis C virus replication and NS3 helicase by the extract of the feather star *Alloeocomatella polycladia*. Mar Drugs 10: 744–761.
40. Fujimoto Y, Salam KA, Furuta A, Matsuda Y, Fujita O, et al. (2012) Inhibition of Both Protease and Helicase Activities of Hepatitis C Virus NS3 by an Ethyl Acetate Extract of Marine Sponge Amphimedon sp. PLoS One 7: e48685.
41. Jin H, Yamashita A, Maekawa S, Yang PT, He LM, et al. (2008) Griseofulvin, an oral antifungal agent, suppresses hepatitis C virus replication in vitro. Hepatology Research 38: 909–918.

JVI
Journals.ASM.org

Japanese Encephalitis Virus Core Protein Inhibits Stress Granule Formation through an Interaction with Caprin-1 and Facilitates Viral Propagation

Hiroshi Katoh,[a] Toru Okamoto,[a] Takasuke Fukuhara,[a] Hiroto Kambara,[a] Eiji Morita,[b] Yoshio Mori,[d] Wataru Kamitani,[c] Yoshiharu Matsuura[a]

Department of Molecular Virology,[a] International Research Center for Infectious Diseases,[b] and Global COE Program,[c] Research Institute for Microbial Diseases, Osaka University, Osaka, Japan; Department of Virology III, National Institute of Infectious Diseases, Tokyo, Japan[d]

Stress granules (SGs) are cytoplasmic foci composed of stalled translation preinitiation complexes induced by environmental stress stimuli, including viral infection. Since viral propagation completely depends on the host translational machinery, many viruses have evolved to circumvent the induction of SGs or co-opt SG components. In this study, we found that expression of Japanese encephalitis virus (JEV) core protein inhibits SG formation. Caprin-1 was identified as a binding partner of the core protein by an affinity capture mass spectrometry analysis. Alanine scanning mutagenesis revealed that Lys^{97} and Arg^{98} in the α-helix of the JEV core protein play a crucial role in the interaction with Caprin-1. In cells infected with a mutant JEV in which Lys^{97} and Arg^{98} were replaced with alanines in the core protein, the inhibition of SG formation was abrogated, and viral propagation was impaired. Furthermore, the mutant JEV exhibited attenuated virulence in mice. These results suggest that the JEV core protein circumvents translational shutoff by inhibiting SG formation through an interaction with Caprin-1 and facilitates viral propagation *in vitro* and *in vivo*.

In eukaryotic cells, environmental stresses such as heat shock, oxidative stress, UV irradiation, and viral infection trigger a sudden translational arrest, leading to stress granule (SG) formation (1). SGs are cytoplasmic foci composed of stalled translation preinitiation complexes and are postulated to play a critical role in regulating mRNA metabolism during stress via so-called "mRNA triage" (2). The initiation of SG formation results from phosphorylation of eukaryotic translation initiation factor 2α (eIF2α) at Ser^{51} by various kinases, including protein kinase R (PKR), PKR-like endoplasmic reticulum kinase (PERK), general control nonrepressed 2 (GCN2), and heme-regulated translation inhibitor (HRI), which are commonly activated by double-stranded RNA (dsRNA), endoplasmic reticulum (ER) stress, nutrient starvation, and oxidative stress, respectively. Phosphorylation of eIF2α reduces the amount of eIF2-GTP-tRNA complex and inhibits translation initiation, leading to runoff of elongating ribosomes from mRNA transcripts and the accumulation of stalled translation preinitiation complexes. Thus, SGs are defined by the presence of components of translation initiation machinery, including 40S ribosome subunits, poly(A)-binding protein (PABP), eIF2, eIF3, eIF4A, eIF4E, eIF4G, and eIF5. Then, primary aggregation occurs through several RNA-binding proteins (RBPs), including T-cell intracellular antigen-1 (TIA-1), TIA-1-related protein 1 (TIAR), and Ras-Gap-SH3 domain-binding protein (G3BP). These RBPs are independently self-oligomerized with the stalled initiation factors and with other RBPs, such as USP10, hnRNP Q, cytoplasmic activation/proliferation-associated protein-1 (Caprin-1), and Staufen and with nucleated mRNA-protein complex (mRNP) aggregations (3, 4). SG assembly begins with the simultaneous formation of numerous small mRNP granules which then progressively fuse into larger and fewer structures, a process known as secondary aggregation (5). The aggregation of TIA-1 or TIAR is regulated by molecular chaperones, such as heat shock protein 70 (Hsp70) (3), whereas that of G3BP is controlled by its phosphorylation at Ser^{149} (4). SG formation and disassembly in response to cellular stresses are strictly regulated by multiple factors.

Viral infection can certainly be viewed as a stressor for cells, and SGs have been reported in some virus-infected cells. Since the propagation of viruses is completely reliant on the host translational machinery, stress-induced translational arrest plays an important role in host antiviral defense. To antagonize this host defense, most viruses have evolved to circumvent SG formation during infection. For example, poliovirus (PV) proteinase 3C cleaves G3BP, leading to effective SG dispersion and virus propagation (6). Influenza A virus nonstructural protein 1 (NS1) has been shown to inactivate PKR and prevent SG formation (7). In the case of human immunodeficiency virus 1 (HIV-1) infection, Staufen1 is recruited in ribonucleoproteins for encapsidation through interaction with the Gag protein to prevent SG formation (8). In contrast, some viruses employ alternative mechanisms of translation initiation and promote SG formation to limit cap-dependent translation of host mRNA (9, 10). In addition, vaccinia virus induces cytoplasmic "factories" in which viral translation, replication, and assembly take place. These factories include G3BP and Caprin-1 to promote transcription of viral mRNA (11).

Japanese encephalitis virus (JEV) belongs to the genus *Flavivirus* within the family *Flaviviridae*, which includes other mosquito-borne human pathogens, such as dengue virus (DENV), West Nile virus (WNV), and yellow fever virus, that frequently cause significant morbidity and mortality in mammals and birds (12). JEV has

Received 15 August 2012 Accepted 15 October 2012
Published ahead of print 24 October 2012
Address correspondence to Yoshiharu Matsuura, matsuura@biken.osaka-u.ac.jp.

doi:10.1128/JVI.02186-12